Earth and Planetary Science Letters 381 (2013) 63–77

Contents lists available at ScienceDirect

Earth and Planetary Science Letters

www.elsevier.com/locate/epsl

Crustal-scale recycling in caldera complexes and rift zones along the Yellowstone hotspot track: O and Hf isotopic evidence in diverse zircons from voluminous rhyolites of the Picabo volcanic field, Idaho

Dana L. Drew [a,*], Ilya N. Bindeman [a], Kathryn E. Watts [b], Axel K. Schmitt [c], Bin Fu [d], Michael McCurry [e]

[a] Department of Geological Sciences, 1272 University of Oregon, Eugene, OR 97403, USA
[b] U.S. Geological Survey, 345 Middlefield Road, Menlo Park, CA 94025, USA
[c] Department of Earth and Space Sciences, University of California, Los Angeles, CA 90095, USA
[d] Research School of Earth Sciences, The Australian National University, Canberra, ACT 0200, Australia
[e] Department of Geosciences, Idaho State University, Pocatello, ID 83209, USA

ARTICLE INFO

Article history:
Received 6 March 2013
Received in revised form 11 July 2013
Accepted 2 August 2013
Available online xxxx
Editor: B. Marty

Keywords:
Picabo
Snake River Plain
oxygen isotopes
caldera
rhyolite

ABSTRACT

Rhyolites of the Picabo volcanic field (10.4–6.6 Ma) in eastern Idaho are preserved as thick ignimbrites and lavas along the margins of the Snake River Plain (SRP), and within a deep (>3 km) borehole near the central axis of the Yellowstone hotspot track. In this study we present new O and Hf isotope data and U–Pb geochronology for individual zircons, O isotope data for major phenocrysts (quartz, plagioclase, and pyroxene), whole rock Sr and Nd isotope ratios, and whole rock geochemistry for a suite of Picabo rhyolites. We synthesize our new datasets with published Ar–Ar geochronology to establish the eruptive framework of the Picabo volcanic field, and interpret its petrogenetic history in the context of other well-studied caldera complexes in the SRP. Caldera complex evolution at Picabo began with eruption of the 10.44 ± 0.27 Ma (U–Pb) Tuff of Arbon Valley (TAV), a chemically zoned and normal-$\delta^{18}O$ ($\delta^{18}O$ magma $= 7.9‰$) unit with high, zoned $^{87}Sr/^{86}Sr_i$ (0.71488–0.72520), and low-$\varepsilon_{Nd}(0)$ (−18) and $\varepsilon_{Hf}(0)$ (−28). The TAV and an associated post caldera lava flow possess the lowest $\varepsilon_{Nd}(0)$ (−23), indicating ~40–60% derivation from the Archean upper crust. Normal-$\delta^{18}O$ rhyolites were followed by a series of lower-$\delta^{18}O$ eruptions with more typical (lower crustal) Sr–Nd–Hf isotope ratios and whole rock chemistry. The voluminous 8.25 ± 0.26 Ma West Pocatello rhyolite has the lowest $\delta^{18}O$ value ($\delta^{18}O_{melt} = 3.3‰$), and we correlate it to a 1,000 m thick intracaldera tuff present in the INEL-1 borehole (with published zircon ages 8.04–8.35 Ma, and similarly low-$\delta^{18}O$ zircon values). The significant (4–5‰) decrease in magmatic-$\delta^{18}O$ values in Picabo rhyolites is accompanied by an increase in zircon $\delta^{18}O$ heterogeneity from ~1‰ variation in the TAV to > 5‰ variation in the late-stage low-$\delta^{18}O$ rhyolites, a trend similar to what is characteristic of Heise and Yellowstone, and which indicates remelting of variably hydrothermally altered tuffs followed by rapid batch assembly prior to eruption. However, due to the greater abundance of low-$\delta^{18}O$ rhyolites at Picabo, the eruptive framework may reflect an intertwined history of caldera collapse and coeval Basin and Range rifting and hydrothermal alteration. We speculate that the source rocks with pre-existing low-$\delta^{18}O$ alteration may be related to: (1) deeply buried and unexposed older deposits of Picabo-age or Twin Falls-age low-$\delta^{18}O$ volcanics; and/or (2) regionally-abundant late Eocene Challis volcanics, which were hydrothermally altered near the surface prior to or during peak Picabo magmatism. Basin and Range extension, specifically the formation of metamorphic core complexes exposed in the region, could have facilitated the generation of low-$\delta^{18}O$ magmas by exhuming heated rocks and creating the large water-rock ratios necessary for shallow hydrothermal alteration of tectonically (rift zones) and volcanically (calderas) buried volcanic rocks. These interpretations highlight the major processes by which supereruptive volumes of magma are generated in the SRP, mechanisms applicable to producing rhyolites worldwide that are facilitated by plume driven volcanism and extensional tectonics.

1. Introduction

Large-volume rhyolitic volcanism in the Snake River Plain (SRP) began at ~16 Ma and migrated from Oregon to Nevada and

* Corresponding author.
E-mail addresses: dld@uoregon.edu (D.L. Drew), bindeman@uoregon.edu (I.N. Bindeman), kwatts@usgs.gov (K.E. Watts), axel@oro.ess.ucla.edu (A.K. Schmitt), bin.fu@anu.edu.au (B. Fu), mccumich@isu.edu (M. McCurry).

0012-821X/$ – see front matter
http://dx.doi.org/10.1016/j.epsl.2013.08.007

through Idaho as the North American plate moved southwest over the Yellowstone hotspot (Fig. 1a; Pierce and Morgan, 1992; Schmandt et al., 2012). High heat fluxes and basalt input from the Yellowstone plume have facilitated large-scale melting of the crust and the formation of unique "SRP-type" rhyolites that are characterized by exceptionally large eruptive volumes, high magmatic temperatures, and anhydrous mineralogies (Branney et al., 2008; Christiansen and McCurry, 2008; Nash et al., 2006). The chemical and isotopic characteristics of SRP rhyolites have been experimentally and numerically modeled to be consistent with mid-crustal generation ($\leqslant$10 km; Almeev et al., 2012; Rodgers and McCurry, 2009) and shallow-level (1–5 km) storage, assembly, and differentiation (Simakin and Bindeman, 2012).

Greater than 10,000 km^3 of rhyolite with low-δ^{18}O values and diverse δ^{18}O zircon populations have erupted across the SRP over the past 16 Ma (Bindeman and Valley, 2001; Bindeman et al., 2007; Cathey et al., 2008; Watts et al. 2011, 2012; our unpublished data). However, the distribution and volume of low-δ^{18}O rhyolites is not homogeneous across the SRP. It appears that less focused magmatism and more frequent silicic eruptions with uniformly low-δ^{18}O values characterize the older Bruneau–Jarbidge (BJ) and Twin Falls (TF) eruptive centers in the central SRP (CSRP) (Bonnichsen et al., 2008; Boroughs et al., 2005; Cathey et al., 2008; Cathey and Nash, 2004; Ellis et al., 2010), in contrast to the younger Heise and Yellowstone centers in the eastern SRP, which are characterized by fewer and larger individual caldera-forming eruptions that create nested caldera complexes with temporal decreases in δ^{18}O (Bindeman et al. 2007, 2008; Watts et al. 2011, 2012).

This paper describes the Picabo eruptive center, which precedes Heise and Yellowstone and postdates BJ-TF in the spatiotemporal progression of the Yellowstone hotspot track (Fig. 1). Picabo produced at least three, but likely six major caldera-forming eruptions from 10.4–6.6 Ma (Table 1). Here we combine detailed isotopic, geochronologic, and geochemical studies using microanalytical methods to elucidate the mechanisms by which Picabo rhyolites were formed, and compare these mechanisms to those proposed for various large-volume rhyolites in the eastern and central SRP.

2. Background

2.1. Defining the Picabo volcanic field

The Yellowstone hotspot track is defined by a spatiotemporal progression of large-volume volcanic fields, and the SRP is considered to be floored by overlapping calderas across its length and width (Fig. 1a; Pierce and Morgan, 1992). However, a thick ($\sim$750 m to 2 km) veneer of Quaternary basalt blankets the Picabo, TF, and BJ volcanic fields (Doherty et al., 1979; Kuntz et al., 1992; Whitehead, 1992), concealing potential caldera ring fractures. The location of the Picabo volcanic field has been approximated on the basis of the outflow distribution of one prevalent unit, the Tuff of Arbon Valley (TAV), shown on Fig. 1, and isostatic gravity, Bouger, and aeromagnetic anomalies (Pierce and Morgan, 1992). Since volcanism has been previously associated with the TAV, the existence of the Picabo volcanic field has been speculative, because the eruption of the TAV was $\sim$150 km east of where the hypothesized locus of the active hotspot is modeled to have been at $\sim$10.5 Ma (Nash et al., 2006). This "early" eruption of the TAV was crystal-rich, biotite-bearing, and possessed a strong Archean upper crustal isotopic signature (Table 1). The TAV is therefore markedly different than crystal poor SRP rhyolites with anhydrous mineralogies and muted upper crustal signatures (Christiansen and McCurry, 2008; McCurry and Rodgers, 2009; Nash et al., 2006). Since the TAV was the only rhyolite previously associated with Picabo, other than those recorded in the airfall record (Anders et al., 2009), the nature, history, and composition of the Picabo eruptive field was poorly constrained and its existence questioned (Nash and Perkins, 2012).

We have now assigned eight lava flows and voluminous ignimbrites of eastern Idaho (Fig. 1.C) with the Picabo volcanic field based on our new and compiled geochronology and proximity to the hypothesized caldera boundary; these include the TAV, Two-and-a-Half-Mile rhyolite, Tuff of Hawley Springs, Tuff of Little Chokecherry Canyon, West Pocatello rhyolite, Tuff of American Falls, Stevens Peak rhyolite, and Stevens Peak 2 rhyolite. In addition, there are a number of tuffs and lavas preserved in two deep geothermal boreholes: the 3.2 km Idaho National Laboratory borehole (INEL-1) and $\sim$1.52 km WO-2 borehole (Anders et al., 2009; Doherty et al., 1979; McCurry and Rodgers, 2009; Shervais et al., 2006). The INEL-1 borehole consists of an upper 650 m of basaltic lava interbedded with alluvium and sediments, underlain by 84 m of tuffaceous silt and clay and a series of devitrified and propyllitically-altered rhyolite tuffs 2.5 km thick (Doherty et al., 1979). Zircons from these rhyolites yielded analytically indistinguishable U–Pb ages of 8.27 ± 0.27, 8.04 ± 0.10, and 8.35 ± 0.24 Ma (with increasing stratigraphic depth; McCurry and Rodgers, 2009). Based on thickness and lithology the rhyolites are presumed to be intracaldera fill (McCurry and Rodgers, 2009). We used the borehole INEL-1 to make isotopic and chemical correlations between intracaldera fill and outflow sheets, in order to further confirm the presence of buried calderas. The WO-2 borehole (5 km southeast of INEL-1) similarly intersected 1.15 km of basalt and 1.23 km of rhyolite (McCurry and Rodgers, 2009; Shervais et al., 2006), however, the rhyolite units (dated at 6.12 Ma and 6.38 Ma; Anders et al., 1997) are in the age range of the Blacktail Tuff of the Heise volcanic field (Morgan and McIntosh, 2005; Morgan et al., 1984), and therefore are not likely derived from Picabo magmatism. Since this borehole did not intersect Picabo rhyolites, we use the location of the borehole to help infer the northern caldera wall boundary (Fig. 1b).

2.2. Local tectonic framework

The SRP is located in the northern Basin and Range province, a region now characterized by east–west extension (Miller et al., 1999; Stockli, 1999). Even prior to extension this region experienced a prolonged history of magmatism and regional folding, from the late Cretaceous through the early Cenozoic (Armstrong, 1982; Burchfiel et al., 1992; DeCelles 1994, 2004). The regional tectonic history modified the crustal architecture prior to hotspot track-related volcanism, affecting the crustal structure and strength (Bonnichsen et al., 2008). Extensional tectonics since $\sim$15–10 Ma (Colgan et al., 2007; Egger et al. 2003, 2010; Fosdick and Colgan, 2008; Wells et al., 2000), have formed extensional basins and detachment systems, and exhumed metamorphic core complexes (Coney, 1980; Foster and Fanning, 1997; Foster et al. 2007, 2010). The Albion–Raft River–Grouse Creek complex is a metamorphic core complex we consider to be of utmost relevance to this study, because it is located on the southern margin of the SRP, in close proximity to the Picabo volcanic field (Fig. 1A). This core complex has also been recently shown to be exhumed beginning at 14 Ma and with faulting continuing to after 8.2 Ma (Konstantinou et al., 2012), both predating and occurring coevally with the development of the Picabo volcanic field. Magmatism accompanying extension includes the Challis-Absaroka and Great Basin volcanics (Armstrong and Ward, 1991; Best and Christiansen, 1991; Christiansen and Yeats, 1992; Gans 1987; Wells and Hoisch, 2008). Volcanism of the Challis-Absaroka province (Fig. 1a) initiated at 51 Ma and continued for $\sim$5 to 10 million years, originally covering over half the state of Idaho with eruptive products (Orr and

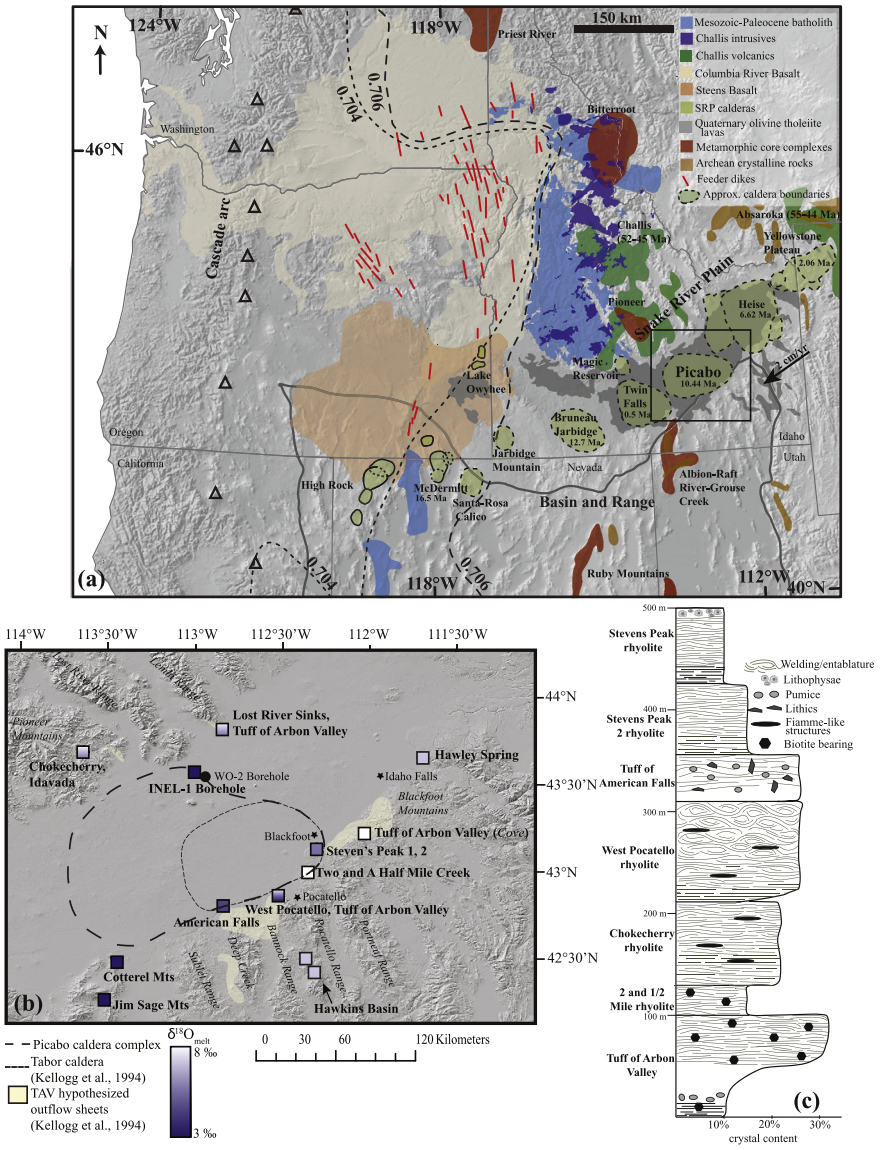

Fig. 1. a. Map of the Snake River Plain volcanic fields and crustal features in the western United States (adopted from the literature, see Appendix 2). The $^{87}Sr/^{86}Sr = 0.706$ defines the transition from Mesozoic–Paleozoic accreted oceanic terranes to Precambrian craton (Farmer and Depaolo, 1983; Fleck and Criss, 1985). **b.** Map showing the Picabo volcanic field in the Snake River Plain and the sampling localities of this study. The approximate boundary of the Tabor caldera, the source of the Tuff of Arbon Valley (TAV), is shown as well as approximate locations of TAV outflow sheets in yellow (Kellogg et al., 1994). The various sampling localities are square symbols with the color of the symbol corresponding to the $\delta^{18}O_{melt}$. Where more than one sample is present at a given locality, a gradient is used to depict the range of $\delta^{18}O_{melt}$. **c.** Generalized stratigraphic section of the Picabo rhyolites analyzed in this study, highlighting the order of eruptions, defining field characteristics, volume percentage of crystals, and approximate thickness. Since the rhyolites are not exposed in the same locations the stratigraphic order is inferred from U–Pb zircon dating, and Ar–Ar and K–Ar ages. (For interpretation of the references to color in this figure legend, the reader is referred to the web version of this article.)

Orr, 1996). Basin and Range extension terminated just north of the current SRP and is thought to have been concentrated south of the SRP during the time of plume-related magmatism (Colgan and Henry, 2009; Egger et al., 2010). However, more evidence has emerged suggesting that extension both predated and was coeval with plume-drive magmatism in the CSRP (Konstantinou et al., 2012; Stockli, 1999), creating conditions for faulting, hydrothermal alteration, and $\delta^{18}O$ preconditioning of the crust prior to SRP volcanism.

2.3. The Tuff of Arbon Valley and rhyolites of the Picabo volcanic field

The rhyolites that constitute the Picabo volcanic field (see Fig. 1 and Table 1) are found ~100 km apart on the northern and southern margins of the SRP as nonwelded and welded ignimbrites, lava flows, airfall, and reworked deposits (unit descriptions in the Appendix). We consider the TAV and West Pocatello rhyolite to be two major caldera-forming eruptions due to their extensive exposures on the surface and/or in the borehole. The other studied rhyolites are more localized due to limited preservation as a result of the highly dissected terrain, and therefore we are unable to locally trace the outflow-sheets or correlate rhyolites between locations. Due to this limited preservation and up to 2 km thick basaltic cover, we place an emphasis on the geochemical and isotopic evolution of the package of outflow deposits rather than field observations and distribution of the individual ignimbrites.

The TAV consists of a lower poorly-welded, crystal-poor (~5%) airfall tuff with pumice, lithics and accretionary lapilli and an upper moderately welded, crystal rich (>35%) tuff (Kellogg et al., 1994). We examined the type locality of the TAV, the Cove (Fig. 1), where >100 m of exposed section of both the upper and lower tuff is preserved (Kellogg et al., 1994). Anders et al. (2009) hy-

pothesized that this unit represents two closely spaced eruptions, $^{40}Ar/^{39}Ar$ dated at 10.34 ± 0.01 and 10.16 ± 0.01 Ma, but our sampling locality at the Cove exhibited no cooling breaks. The source of the TAV is thought to be the Tabor caldera (Fig. 1; Kellogg et al., 1994), due the thickness and presence of full stratigraphic sections at the southern margin of the plain (McCurry, 2009) and observations that the ignimbrites thin to the south from the proposed caldera boundary. The Two-and-a-Half Mile rhyolite is geochemically and petrographically similar to the TAV, located along the eastern margin of the Tabor caldera. Picabo's subsequent eruptions (Table 1) produced more densely welded, crystal poor (5–25%) rhyolites similar to classic "SRP type" ignimbrites (Branney et al., 2008). For example, the voluminous West Pocatello rhyolite is a densely welded ignimbrite (25 vol% phenocrysts) that is laterally extensive, capping mountains south of Pocatello.

3. Methods

Individual zircon cores were analyzed for $\delta^{18}O$ and ^{238}U–^{206}Pb ages (25–30 μm lateral resolution and <1 μm depth resolution) using the CAMECA ims 1270 ion microprobe at UCLA. Analytical reproducibility was estimated from the standard deviation (s.d.) of replicate analyses of KIM-5 (5.09‰; Valley, 2003) and AS3 (5.34‰; Trail et al., 2007) standard zircons on the same mount, in close spatial proximity to the unknowns. In three analytical sessions these values were 0.38‰ ($n = 54$), 0.27‰ ($n = 12$), and 0.14‰ ($n = 31$). Accuracy was checked through intercalibration of KIM-5 and AS3, whose averages were found to agree within 0.2‰. Zircon spots analyzed on the ion microprobe were later analyzed for $^{176}Hf/^{177}Hf$ at the Australian National University, Canberra on a 193 nm excimer laser-based HELEX ablation system with a Neptune multiple-collector ICPMS as described in Eggins et al. (2005) (a few additional zircons were analyzed at Washington State University on a Finnigan Neptune MC-ICP-MS). The laser spot dimensions were 37 μm in lateral dimensions, and the ablation time was 60 s for each analysis (protocols from Woodhead et al., 2004). The $^{176}Hf/^{177}Hf$ data was reduced offline using the software package Iolite (e.g., Paton et al., 2011).

Oxygen isotope ratios of quartz, plagioclase, and pyroxene phenocrysts were measured by laser fluorination at the University of Oregon using methods described by Bindeman (2008). BrF_5 was the reagent used, and an overall precision of <0.1‰ was achieved for individual analytical sessions. Major and trace elements were analyzed by XRF of whole rock powders at the GeoAnalytical Laboratory at WSU. Whole rock Sr and Nd isotope analyses were conducted on a Sector 54 thermal ionization mass spectrometer (TIMS) at the University of New Mexico. A more detailed treatment of the methods is included in the Appendix.

4. Results

Below we describe the geochemistry, geochronology, and isotopic ratios of whole-rock and individual phenocrysts of a suite of rhyolites derived from the SRP. We highlight the compositional evolution of these rhyolites through time, which we later use to interpret rhyolite petrogenesis and magma assembly.

4.1. Geochronology of Picabo ignimbrites and lavas

Our U–Pb dating of zircon cores from six ignimbrites (Table 1) establishes that the duration of volcanism at the Picabo volcanic field is 10.44–6.62 Ma. Comparison of these U/Th disequilibria-corrected U–Pb ages with published Ar–Ar and K–Ar ages (Anders et al., 2009; Kellogg and Marvin, 1988, Kellogg et al., 1994) indicate that the majority of Picabo zircon populations are within uncertainty of the Ar–Ar age for samples where eruption ages are available (TAV, West Pocatello rhyolite and Tuff of American Falls).[1]

We also studied the following newly identified units (Table 1, Appendix Table A3.3): Idavada biotite-bearing trachydacites (>9.34 Ma; Ar–Ar dated by Anders et al., 2009), Jim Sage and Cotterel Mountain rhyolites (9.5–8.2 Ma; U–Pb dated by Konstantinou et al., 2012), and the Hawkins Basin volcanics (6.63–6.09 Ma; U–Pb dated by Pope, 2002).

4.2. Isotopic and compositional evolution: $\delta^{18}O$, $^{87}Sr/^{86}Sr$, $^{143}Nd/^{144}Nd$ and $^{176}Hf/^{177}Hf$

Studied Picabo samples are largely metaluminous low- to high-silica (74–77% SiO_2) rhyolites (Table A3.1) with a range in crystal content of <5 to 35 volume % phenocrysts (Table A3.2) and liquidus temperatures of 850 °C on average (estimated using rhyoliteMELTS) (Fig. A5.1). The mineral assemblage is dominated by plagioclase, alkali feldspar, clinopyroxene, orthopyroxene, Fe–Ti oxides, ±quartz, ±biotite/hornblende, and ±accessory zircon (Table A3.2). Variations in major and trace element whole rock geochemistry (Table A3.1) between individual rhyolites is largely governed by fractionation of this mineral assemblage (Fig. 2, 3a), and demonstrates a general enrichment in high field strength elements and an A-type granite signature (Fig. 3b). Picabo rhyolites span a $\delta^{18}O_{melt}$ range from 8.3 to 2.1‰ and a $\delta^{18}O_{zircon}$ range of 6.80 to 0.01‰ (Fig. 6). Major phases of quartz and plagioclase display small ranges in $\delta^{18}O$ within samples, suggesting equilibrium at magmatic temperatures and therefore magmatic $\Delta^{18}O_{melt\text{-}plag}$ and $\Delta^{18}O_{melt\text{-}quartz}$ (Fig. 5), which were used to calculate $\delta^{18}O_{melt}$.[2]

Volcanism initiated with the normal-$\delta^{18}O$ ($\delta^{18}O_{melt} = 7.9$‰) TAV (10.44 Ma), which exhibits upper crustal characteristics in that it has an extremely low-$\varepsilon_{Nd}(0)$ (−17.7) and $-\varepsilon_{Hf}(0)$ (−28) (Table 1). The TAV possesses large vertical zonation from high-silica rhyolite at the base to low-silica rhyolite at the top. This transition in SiO_2 is coupled with significant zoning in $^{87}Sr/^{86}Sr_i$ from 0.72520 in the Sr-poor lower tuff to 0.71488 in the upper tuff, demonstrating dramatic compositional changes within a single eruption (Fig. 4a, b; Table A3.1). However, there is < 0.4‰ difference in the average $\delta^{18}O_{melt}$ between the base and top of the section, which is <1‰ variation observed within the individual samples of the TAV. Similarly, we observed only a small difference in $\varepsilon_{Nd}(0)$ from the base (−17.7) to the top (−18) of the tuff (Fig. 4c), suggesting negligible zoning in $\delta^{18}O$ and $\varepsilon_{Nd}(0)$ in our analyzed samples. However, Nash et al. (2006) reports an $\varepsilon_{Nd}(0)$ of −19, which suggests the presence of minor zoning in ε_{Nd} (∼−17.7 to 19) of the TAV. Both the ∼9.1 Ma Two-and-a-Half Mile rhyolite and Tuff of Hawley Spring are similarly normal-$\delta^{18}O$ rhyolites ($\delta^{18}O_{melt} = 7.7$‰, 7.1‰ accordingly) with extremely low-$\varepsilon_{Nd}(0)$ (−23, −30.9 accordingly). Due to the similarities in the TAV, Two-and-a-Half-Mile rhyolite, and Tuff of Hawley Spring, we consider the Two-and-a-Half-Mile rhyolite to be a post-TAV lava flow de-

[1] Notable exceptions are the Tuff of Lost River Sinks and the rhyolite of Stevens Peak, which have significantly older Ar–Ar/K–Ar ages that do not overlap our determined U–Pb ages. The K–Ar age of the Stevens Peak rhyolite was likely inaccurate and an updated Ar–Ar age would be expected to be in agreement with the reported U–Pb age. The Tuff of Lost River Sinks we sampled was likely the Blacktail Creek Tuff and therefore demonstrates agreement with an Ar–Ar age of 6.63 ± 0.03 Ma (Morgan and McIntosh, 2005).

[2] The fractionation factor between individual quartz phenocrysts and melt is derived from a linear correlation with temperature (Bindeman and Valley, 2003), while the plagioclase fractionation factor is dependent on a linear correlation with SiO_2 (Valley et al., 2003). In samples where quartz was the dominant phenocryst phase, TAV and Two and a Half Mile rhyolite, a Δ (quartz-melt) of 0.5‰ was used, corresponding to a temperature of ∼800 °C. For all other samples where plagioclase was the dominant phenocryst, a Δ (plagioclase-melt) was calculated and was ∼ − 0.57‰ for 73–77% SiO_2.

Table 1
Ages and compositions of Picabo ignimbrites and lavas in this study. The $^{206}Pb/^{238}U$ concordia ages have been disequilibrium corrected and are shown with 95% confidence intervals. Ar–Ar and K–Ar (italicized) ages are included for comparison. The zircon $\delta^{18}O$ range of individual zircon core measurements (zrc range) is presented with a one-sigma standard deviation (see the supplementary material for individual zircon data). The $\delta^{18}O$ value of quartz (qtz), plagioclase (plag), and pyroxene (pyrx) is also reported. The $\delta^{18}O_{melt}$ composition was calculated from the quartz and plagioclase phenocryst $\delta^{18}O$ measured compositions and from known fractionation factors between the mineral and melt for the average temperature of 850 °C (Bindeman and Valley, 2003). Liquidus temperatures (liq) represent the first appearance of feldspar or quartz, and were calculated using rhyolite MELTS at a pressure of 1.5 kilobars, 3-wt% H_2O (using a water content of 1.5 wt% would shift temperatures upwards by ~50 °C), and QFM oxygen fugacity. Zircon saturation temperatures (zrc sat) were calculated from whole rock compositions, specifically major elements and zirconium (Miller et al., 2003; Hanchar and Watson, 2003). $\varepsilon_{Hf}(0)$ is the current ε_{Hf} ($t = 0$) (see Appendix for $\varepsilon_{Hf}(t)$ of the ε_{HF} at the time of formation).

Unit	Sample	Abbr.	K/Ar–Ar age (Ma)	U–Pb age (Ma)	$\delta^{18}O$ (‰)				$\delta^{18}O_{melt}$ (‰)	Temp (°C)		$^{86}Sr/^{87}Sr_i$	$^{86}Sr/^{87}Sr$	$^{143}Nd/^{144}Nd$	$\varepsilon_{Nd}(0)$	$\varepsilon_{Hf}(0)$
					Qtz	Plag	Pyrx	Zrc Range		Zrc Sat	Liq					
*Tuff of Arbon Valley (upper)	PC-14	TAV_U	10.2[a]	10.44 ± 0.27	8.41	7.8	–	5.43–6.80	7.9	835	877	0.7252	0.71507	0.51171	−18	−28
*Tuff of Arbon valley (lower)	PC-12	TAV_L	–	–	8.83	7.86	–	–	8.3	754	842	0.71488	0.73443	0.51173	−17.7	–
*Tuff of Little Chokecherry Canyon	PC-71	CC	9.34[a]	9.7 ± 0.12	–	4.2	3.47	0.98–2.00	4.8	860	832	–	–	–	–	−7.7
Two and a Half Mile Rhyolite	PC-20	TFM	*9.1*[b]	–	8.08	–	–	–	7.7	765	827	0.71948	0.72078	0.51145	−23.2	–
*INEL 3686'	INEL-1	INEL	–	8.31 ± 0.22, 8.27 ± 0.27[e]	4.73	1.61	–	0.01–2.51	2.1	861	856	0.71234	*0.71234*[e]	*0.51231*[e]	−6.2	–
*West Pocatello rhyolite	PC-01	PR	*7.9*[c]	8.25 ± 0.26	–	2.79	2.35	0.97–2.75	3.3	877	833	0.71169	0.71231	0.5123	−6.5	−5.5
Tuff of American Falls	PC-34	TAF	7.53[a]	7.91 ± 0.16	5.81	3.74	2.62	0.83–4.77	4.1	888	916	0.71197	0.71218	0.51229	−6.9	−5.7
Hawley Spring	PC-76	HS	*7.2*[d]	–	7.61	–	–	4.30–5.90	7.1	806	842	–	–	–	–	−31.5
Tuff of Lost River Sinks	PC25	TLSR	8.81[a]	7.05 ± 0.13	–	6.22	–	4.08–5.73	6.8	837	816	0.71204	0.71276	0.51211	−10.3	−11.8
Rhyolite of Steven's Peak 2	PC-19	SP2	–	6.86 ± 0.19	–	4.14	–	1.30–6.44	4.7	862	859	0.71052	0.71094	0.51224	−7.8	−9.7
Rhyolite of Steven's Peak	PC-16	SP	*9.8*[b]	6.62 ± 0.12	–	5.37	–	2.73–5.32	5.9	813	816	0.70994	0.712	0.51225	−7.6	−9.5
Lower Jim Sage	PC-62	JS	–	9.46 ± 0.09–9.44 ± 0.10[f]	–	2.27	–	–	2.8	856	853	–	–	–	–	–
Upper Jim Sage	PC-63	JS	–	8.21 ± 0.15[f]	–	3.47	–	–	4	874	834	–	–	–	–	–

[a] Denotes Ar–Ar age from Anders et al. (2009).
[b] Denotes K–Ar age from Kellogg et al. (1994).
[c] Denotes K–Ar age from Kellogg and Marvin (1988).
[d] Denotes K–Ar age from Morgan et al. (1984).
[e] Denotes U–Pb age and data from McCurry and Rodgers (2009).
[f] Denotes U–Pb age from Konstantinou et al. (2012).
[*] Denotes the major caldera-derived ignimbrites.

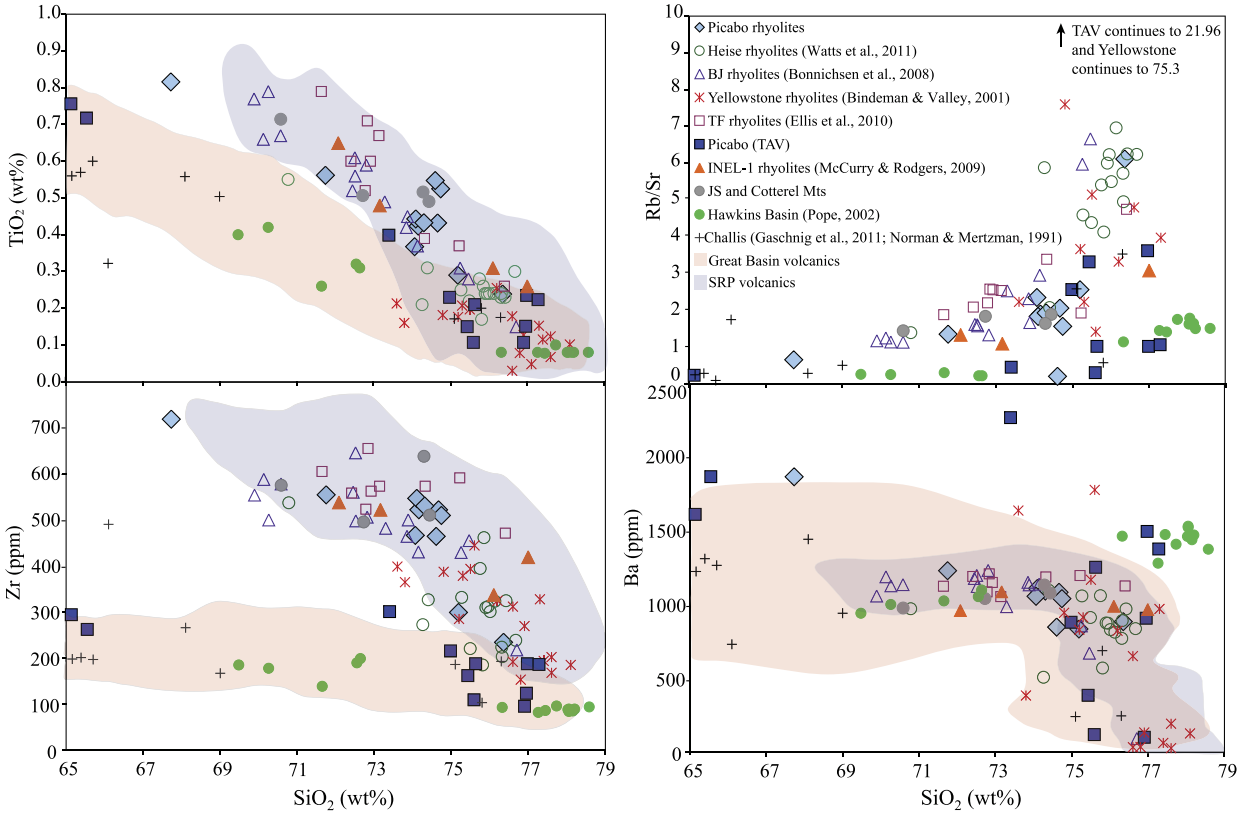

Fig. 2. Whole rock geochemistry plots of Picabo rhyolites, surrounding volcanic center rhyolites: Bruneau–Jarbidge, Twin Falls, Heise and Yellowstone, INEL-1 borehole rhyolites, Jim Sage and Cotterel Mountain rhyolites, Hawkins Basin volcanics, and Challis intrusives. Fields of the Oligocene Great Basin volcanics and range of Snake River Plain compositions are shown for comparison. The Great Basin–Challis volcanics are wet, oxidizing and are derived from subduction processes (Christiansen and McCurry, 2008), which greatly contrasts with the dry and reducing conditions of Snake River Plain rhyolites.

rived from the proposed caldera ring fracture, and the Tuff of Hawley Spring to be a TAV outflow deposit.

On the northern side of the plain the oldest Idavada units (1 through 3) underlying the Tuff of Little Chokecherry Canyon (9.3 Ma), but overlying Eocene Challis volcanics, also have normal $\delta^{18}O_{melt}$ values of 7.0‰, 6.9‰ and 6.6‰, respectively. We propose that these rhyolites are related to the TAV due to the presence of biotite and low $\varepsilon_{Nd}(0)$ (−14.5). The overlying 9.3 Ma Tuff of Little Chokecherry Canyon rhyolite has a lower $\delta^{18}O_{melt}$ value of 4.8‰ and a primitive $\varepsilon_{Hf}(0)$ of −7.7.

The sequence of eruptions that followed includes the voluminous 8.25 Ma West Pocatello rhyolite and the 7.91 Ma Tuff of American Falls. The West Pocatello rhyolite possesses the lowest $\delta^{18}O_{melt}$ value (3.3‰) and highest $\varepsilon_{Nd}(0)$ (−6.5) and $\varepsilon_{Hf}(0)$ (−5.5) found at the Picabo volcanic field (Fig. 4c). We correlate the West Pocatello rhyolite to a rhyolite of the INEL-1 borehole based on nearly identical $\varepsilon_{Nd}(0)$ (−6.5 and −6.2) and zircon U–Pb ages (8.25 ± 0.26, 8.27 ± 0.27, respectively).[3] We consider these units to be coeval extracaldera and intracaldera parts of the same voluminous low-$\delta^{18}O$ eruption. The dacitic Tuff of American Falls is comparable to the West Pocatello rhyolite (within U–Pb dating error) in that is has low-$\delta^{18}O_{melt}$ (4.1‰), and primitive $\varepsilon_{Nd}(0)$ (−6.87) and $\varepsilon_{Hf}(0)$ (−5.7) (Fig. 2, Table A3.1).

The three youngest Picabo units (7.05–6.62 Ma; Table 1), the Tuff of Lost River Sinks, Stevens Peak rhyolite, and a newly identified unit, Stevens Peak 2, have moderately low and distinct $\delta^{18}O_{melt}$ values (5.0‰, 5.9‰, and 4.7‰, respectively), which are higher than the West Pocatello rhyolite (Figs. 5, 6a, b). Each of these three units has subtle differences in $\delta^{18}O$ and U–Pb age of zircons, and critical differences in whole rock chemistry, mineralogy and Sr–Nd–Hf isotopic values (Table 1) that provides evidence that these samples represent distinct eruptions (Tables A3.1, A3.2). Stevens Peak 2 and Stevens Peak rhyolites have relatively primitive $\varepsilon_{Nd}(0)$ signatures of −7.8 and −7.6, respectively as well as primitive $\varepsilon_{Hf}(0)$ of −9.7 and −9.5, respectively.

We found that the 7.05 Ma Tuff of Lost River Sinks displays striking similarities to the Blacktail Creek Tuff of the younger Heise volcanic center in zircon U–Pb ages, normal-$\delta^{18}O$ melt and zircon compositions (Fig. 6a), whole rock geochemistry, $^{87}Sr/^{86}Sr_i$ (0.00034 difference), and ε_{Nd} (0.55 difference). We do observe minor mineral abundance differences on the order of 5%; however, the phenocryst identities and morphologies are very similar. Due to the isotopic and chemical similarities in the Blacktail Creek Tuff of the Heise volcanic center and the Tuff of Lost River Sinks we consider these units to be related, and therefore we do not associate the Lost River Sinks rhyolite with Picabo volcanism. The Tuff of Lost River Sinks also underlies the Blacktail Creek Tuff at the sampling locality, further supporting that these rhyolites are related.

The thick (~1 km) suite of rhyolitic lavas and a thin capping ignimbrite exposed in the Jim Sage and Cotterel Mountains (Fig. 1) (Covington, 1983; Konstantinou et al., 2012; Pierce et al., 1983) were found to have low-$\delta^{18}O_{melt}$ values (Jim Sage melt: 2.8 to 4.0‰; Cotterel Mt: 3.0‰). We also note that the trace and major element characteristics of the Jim Sage and Cotterel Mt. volcanics fall within the SRP rhyolite range (Fig. 2). On the southeast side of the proposed Picabo caldera we found the Hawkins Basin rhyolites

[3] Although INEL-1 3686' and the West Pocatello rhyolite are isotopically similar there are differences in the whole rock geochemistry (MgO, MnO, CaO, Na_2O and K_2O), which we attribute to intracaldera hydrothermal alteration and recrystallization inside the INEL-1 samples.

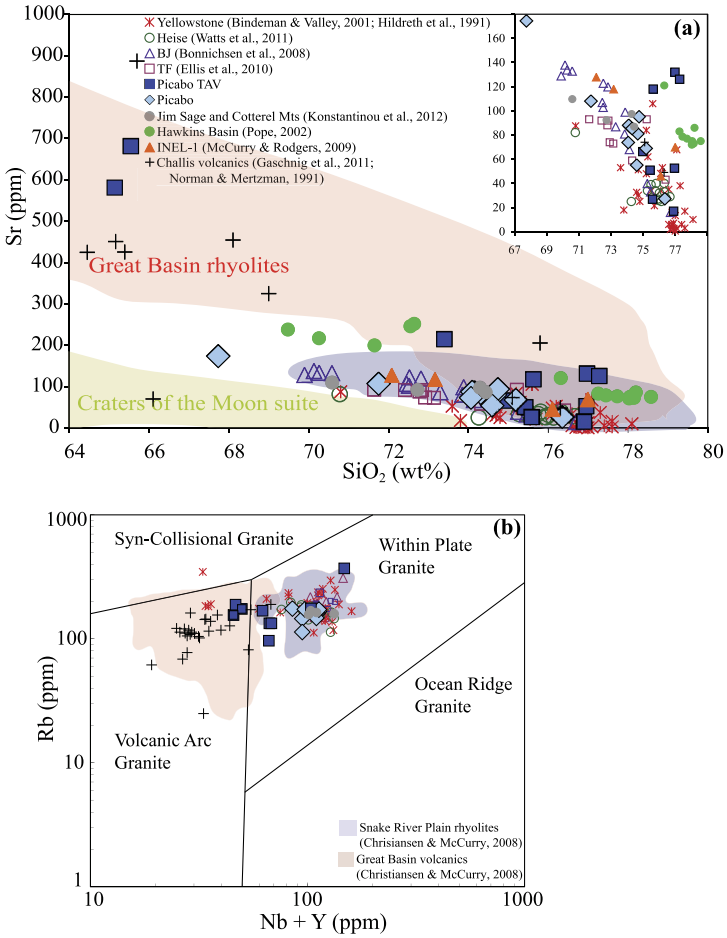

Fig. 3. a. Strontium variation with SiO_2 for Picabo rhyolites, Jim Sage and Cotterel Mt. rhyolites, Hawkins Basin volcanics, and Challis volcanic and intrusives, in comparison to typical Snake River Plain rhyolites and western U.S. volcanics: Quaternary Craters of the Moon volcanic suite and Oligocene Great Basin rhyolites (modified from Christiansen and McCurry, 2008). The Sr-rich nature of the Great Basin volcanics is a result of wet conditions suppressing plagioclase crystallization. **b.** Discriminant diagram of Rb versus Nb + Y for different fields of granite to demonstrate how Snake River Plain rhyolites consistently have a within plate geochemical signature (discriminant diagram of Pearce et al., 1984; modified from Christiansen and McCurry, 2008).

(6.09–6.63 Ma; Pope, 2002) to have normal $\delta^{18}O_{melt}$ values (6.8 to 7.4‰). These rhyolites demonstrated significantly different trends in Zr, Ba, Rb/Sr, and K_2O with SiO_2 than the majority of compiled Picabo, Heise, BJ, TF and Yellowstone samples indicating contrasting fractionation trends (Fig. 2, Figs. A5.3a–c). We do not consider the Hawkins Basin volcanics to be related to Picabo volcanism.

4.3. Heterogeneous $\delta^{18}O$ in zircons

High-resolution $\delta^{18}O$ analyses of zircon cores were compared within individual samples, between samples, and to major phenocryst $\delta^{18}O$ compositions. As previously mentioned, major phenocrysts (quartz and plagioclase) display homogeneous $\delta^{18}O$ and are in equilibrium with the melt, however the TAV is one exception in that quartz $\delta^{18}O$ values were found to be variable up to ~ 1‰ (within an individual TAV sample). Zircons on the other hand display appreciable heterogeneity within individual samples indicating magmatic disequilibrium (Fig. 6b).

As shown in Fig. 6a, the most significant trends in $\delta^{18}O_{melt}$ are the lowering from the 8.3‰ TAV to the 3.3‰ West Pocatello rhyolite, with a subtle recovery in $\delta^{18}O$ in the waning stages. The initial decrease and later recovery in $\delta^{18}O$ through time also corresponds to an increase in $\delta^{18}O_{zircon}$ heterogeneity from ~ 1‰ variation in the TAV up to 5‰ in the lower $\delta^{18}O$ units. The two xenocrystic zircons that are 1.3 million years older than the main zircon population have the same normal-$\delta^{18}O_{zirc}$ composition. The other five Picabo rhyolites have larger $\delta^{18}O_{zirc}$ ranges of 1.6–5.1‰ within individual samples, which is well outside the 2σ-reproducibility for a homogeneous zircon standard (~ 0.5‰). Stevens Peak 2 has the greatest variability in $\delta^{18}O_{zirc}$ (1.3 to 6.4‰), with the majority of zircons from 2.4 to 4.4‰. The two inherited zircons are 1.42 million years older, but are within the same normal $\delta^{18}O$ range as the primary magmatic zircon population.

5. Discussion

5.1. Defining the existence of unexposed calderas at Picabo

We use the following lines of evidence to support the existence of nested calderas in the Picabo volcanic field, which allows us to interpret and characterize the geochemical evolution of the series of eight ignimbrites and lavas we have associated with Picabo (Table 1):

(1) Several thick (10's to >100 m) ignimbrite outflow-sheets with great spatial extent at the northern and southern margins of the plain, with ages between 10.4 and 6.6 Ma.
(2) Geochemical and geochronological correlation of one 8.25 Ma Picabo ignimbrite, the West Pocatello rhyolite, with a 1000 m thick intracaldera fill from the INEL-1 borehole.
(3) Unique geochemical and isotopic compositions of dated Picabo rhyolites in comparison to contemporaneous eruptions

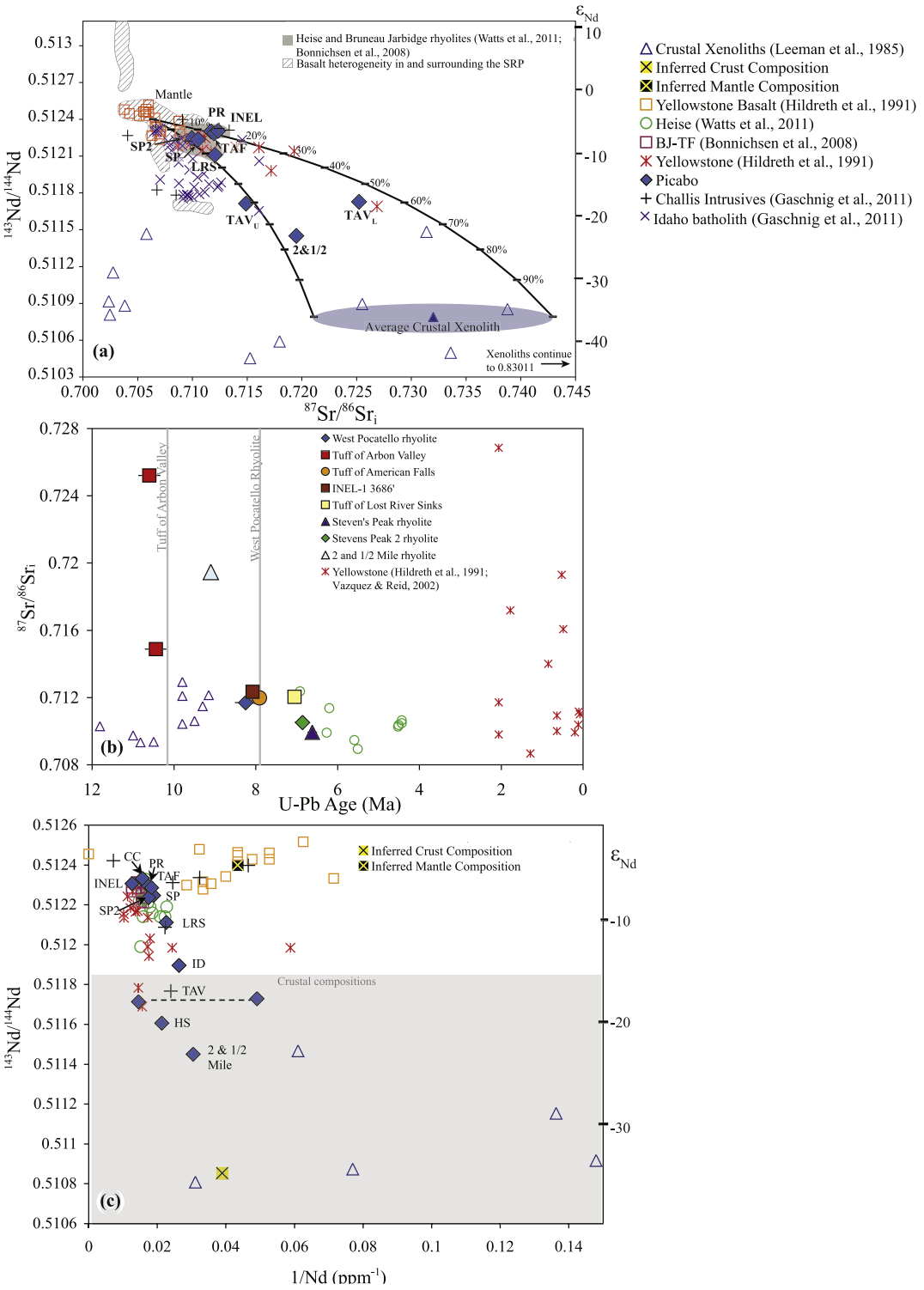

Fig. 4. a. Binary mixing model of $^{87}Sr/^{86}Sr_i$ versus $^{143}Nd/^{144}Nd$ of Picabo rhyolites, in comparison to surrounding eruptive centers (Heise, Yellowstone and Bruneau–Jarbidge), Challis intrusives ($^{87}Sr/^{86}Sr_{t=9\,Ma}$), Idaho batholith ($^{87}Sr/^{86}Sr_{t=9\,Ma}$) and crustal xenoliths. $^{87}Sr/^{86}Sr$, $^{143}Nd/^{144}Nd$, Sr, and Nd crustal xenolith data from Leeman et al. (1985) was averaged and one standard error in $^{87}Sr/^{86}Sr$ was used for the crustal end-members for the binary mixing lines. The average composition of $^{87}Sr/^{86}Sr$, $^{143}Nd/^{144}Nd$, Sr, and Nd is 0.73199±0.01091, 0.51079±0.000113, 347.16, and 18.22 accordingly. The Sr and Nd data of Yellowstone basalts (Hildreth et al., 1991) was averaged and a composition of 0.7063, 0.5124, 300 ppm, and 23 ppm accordingly, was used to represent the primitive SRP end-member. The basalt field demonstrates the variability in basalt throughout the Snake River Plain (includes data from Camp and Hanan, 2008; Hughes et al., 2002; Graham et al., 2009). **b.** $^{87}Sr/^{86}Sr$ of Picabo, Heise, and Bruneau–Jarbidge/Twin Falls rhyolites through time. Gray lines are Ar–Ar ages (Anders et al., 2009; Kellogg et al., 1994) of the Tuff of Arbon Valley, Pocatello Rhyolite and Tuff of American Falls. The two points for the Tuff of Arbon Valley are representative of the lower and upper tuff and demonstrate the large vertical isotopic zoning. U–Pb age error bars are one standard error. **c.** $^{143}Nd/^{144}Nd$ versus 1/Nd of Picabo and surrounding volcanic centers in comparison to Yellowstone basalts, Archean crustal xenoliths, and Challis intrusives. The gray field represents the approximate range of Archean crust in $^{143}Nd/^{144}Nd$ (McCurry and Rodgers, 2009).

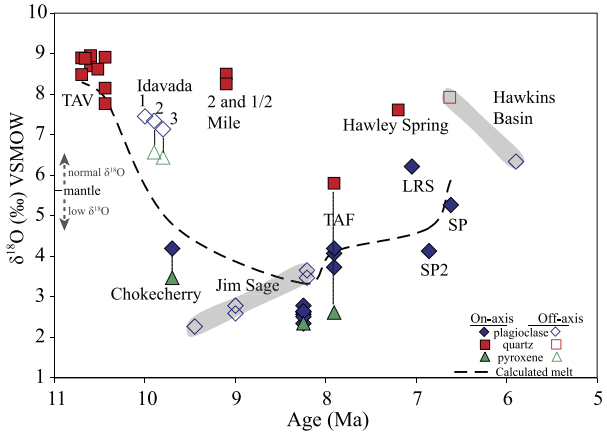

Fig. 5. $\delta^{18}O$ compositions of major phenocryst phases: quartz, plagioclase and pyroxene, and calculated melt $\delta^{18}O$ values versus U–Pb, Ar–Ar or K–Ar age. Filled symbols correspond to the main rhyolites used to define the Picabo volcanic field while open symbols represent samples of approximate Picabo age, but whose association with the Picabo volcanic field is poorly constrained, these include: Hawkins Basin (Pope, 2002), Jim Sage (Konstantinou et al., 2012), and Idavada volcanics. The Two-and-a-Half-Mile rhyolite and Hawley Springs rhyolite are plotted against K–Ar dates (Kellogg and Marvin, 1988 and Morgan et al., 1984 respectively). The Idavada volcanics and middle Jim Sage member ages are approximated based on stratigraphic succession. The $\delta^{18}O_{melt}$ curve is calculated from the TAV quartz $\delta^{18}O$ and the West Pocatello rhyolite, Tuff of American Falls, Stevens Peak and Stevens Peak 2 plagioclase $\delta^{18}O$.

from surrounding volcanic fields to the west (BJ–TF) and east (Heise).

5.2. Petrogenetic implications of the geochemical and isotopic data

In order to assess the petrogenesis of large-volume, isotopically-distinct magmas erupted from the Picabo volcanic field of the eastern SRP, we use a suite of stable and radiogenic isotopic data to quantify the proportions of the mantle, lower crust, and upper Archean and hydrothermally-altered crust in Picabo rhyolites.

Volcanism began at the Picabo volcanic field with the eruption of the normal-$\delta^{18}O$ TAV, with extremely radiogenic Sr and less radiogenic Nd and Hf isotope ratios (Figs. 4a–c, 7a), supporting derivation from melting of significant portions (~50–60%) of upper continental crust (Fig. 4a). This upper crustal contribution to the TAV is ~20–30% greater than is estimated for the majority of other Picabo units, as well as BJ-TF and Heise rhyolites (Fig. 4a,b). Given the highly radiogenic $^{87}Sr/^{86}Sr$ of the TAV and the Two-and-a-Half-Mile rhyolite, and the strong contrast in Sr isotopes between the lower and upper TAV, variable proportions as well as variable end-member compositions of isotopically diverse upper Archean crust are required. The presence of biotite also suggests that the TAV had a lower magmatic temperature, and amphibole geobarometry indicates that crystallization occurred at ~300 MPa corresponding to a depth of ~10 km (McCurry, 2009). Owing to its extreme crustal signature, we speculate that the TAV was either generated prior to the direct passage of the plume, leading to a lower magma flux, which would enable crustal assimilation to greatly overpower the isotopic composition of SRP basalt and/or that the magma reservoir was isolated (perhaps partially or fully crystalline) from later Picabo eruptions.

The majority of eruptions following the TAV were low-$\delta^{18}O$, and all possess more primitive radiogenic isotopic signatures, requiring a greater proportion of lower to mid crust and basaltic magma. Christiansen and McCurry (2008) demonstrated that partial melting of gabbro rather than upper crustal rocks or lower crustal granulite can better reproduce trace element signatures (Rb, Th, U, and Pb) of most SRP rhyolites. However, the moderately elevated $^{87}Sr/^{86}Sr_i$ of all Picabo rhyolites also suggests these magmas sampled a greater portion of Archean crust than surrounding centers (Fig. 4b). The 9.7 Ma Tuff of Little Chokecherry Canyon and 9.44 Ma Jim Sage rhyolite (Konstantinou et al., 2012) are low-$\delta^{18}O$, and there is evidence for low-$\delta^{18}O$ zircons of 9.43 ± 0.36 Ma (Fig. 6a) indicating that low-$\delta^{18}O$ volcanism started between 9.7 and 9.4 Ma, $\leqslant$1 million years after the eruption of the TAV.

The West Pocatello rhyolite and Tuff of American Falls were sourced from a magma reservoir containing entrained xenocrystic zircons (1035 and 580 Ma) and zircons derived from pure crustal melts with extreme $\varepsilon_{Hf}(0)$ as low as -38 (Fig. 7), further corroborating evidence that the later Picabo rhyolites received upper crustal input, although the isotopic signature reflects an overwhelming basaltic component. The later eruptions, Stevens Peak and Stevens Peak 2 rhyolites, were also relatively isotopically primitive, and possess $\delta^{18}O$ higher than the West Pocatello rhyolite, suggesting that observed isotopic trends are not uniform throughout the eruptive sequence and after the initial lowering of $\delta^{18}O$ there is recovery to more elevated $\delta^{18}O$ and lower $\varepsilon_{Hf}(0)$.

5.3. Mechanisms of generating low-$\delta^{18}O$ rhyolites at the Picabo volcanic field

With the discovery of abundant low-$\delta^{18}O$ rhyolites at Picabo, it now appears that the presence of voluminous low-$\delta^{18}O$ rhyolites characterizes nearly all caldera complexes in the SRP. Bindeman et al. (2008) and Watts et al. (2011) proposed that the process for generating Yellowstone and Heise low-$\delta^{18}O$ rhyolites is nested caldera collapse, with repeated caldera formation (at least two nested calderas) creating conditions for hydrothermal alteration and subsequent remelting of buried intracaldera tuffs. This mechanism of bulk cannibalization of erupted pyroclastic rocks leads to the formation of voluminous low-$\delta^{18}O$ rhyolites at the end of caldera cluster evolution in the eastern SRP. In the CSRP, persistently low-$\delta^{18}O$ volcanism from the exposed inception of volcanic activity has led Boroughs et al. (2005, 2012) to advocate that the low-$\delta^{18}O$ signatures in the CSRP predate volcanism and are derived from hydrothermally altered crustal material from the Idaho batholith. However, the vast majority of the Idaho batholith and Archean crustal rocks in the SRP are high-$\delta^{18}O$ (Criss and Fleck, 1987; King and Valley, 2001), and thus are an unlikely source of voluminous low-$\delta^{18}O$ magmatism. The Idaho batholith is also too far west of the Picabo volcanic field (Fig. 1a) to have provided a crustal source for Picabo magmas.

There is compelling geologic evidence (i.e., spatial distribution) that both the TAV, Chokecherry Canyon rhyolite, and West Pocatello rhyolite were formed as a result of caldera collapse in the SRP. However, whether a caldera formed between the TAV and the Tuff of Little Chokecherry Canyon remains unknown. The presence of older normal-$\delta^{18}O$ units followed by low-$\delta^{18}O$ units at Picabo seemingly supports the genesis of low-$\delta^{18}O$ magmas at Picabo by the nested caldera model proposed for Heise and Yellowstone. In this scenario, hydrothermally altered intracaldera TAV is the source of later low-$\delta^{18}O$ melts. However, the "upper crustal" geochemical characteristics of the TAV would require at least 50% dilution by SRP basalt to justify the more primitive radiogenic isotopic signature of later erupted, low-$\delta^{18}O$ units (Fig. 4a). In addition, the lack of intermediate $\delta^{18}O$ values between the TAV and Chokecherry Canyon–West Pocatello rhyolites presents mass balance challenges because it is unknown whether intracaldera TAV reached sufficient depths to be remelted at the time of the first low-$\delta^{18}O$ magma genesis. While this is not inconceivable, an alternative explanation is that the voluminous 9–7 Ma low-$\delta^{18}O$ volcanism at the Picabo volcanic field shares some similarities with the "persistent" low-$\delta^{18}O$ volcanism at the BJ–TF centers to the west (Fig. 6a) (Cathey and Nash, 2009; Seligman, 2011).

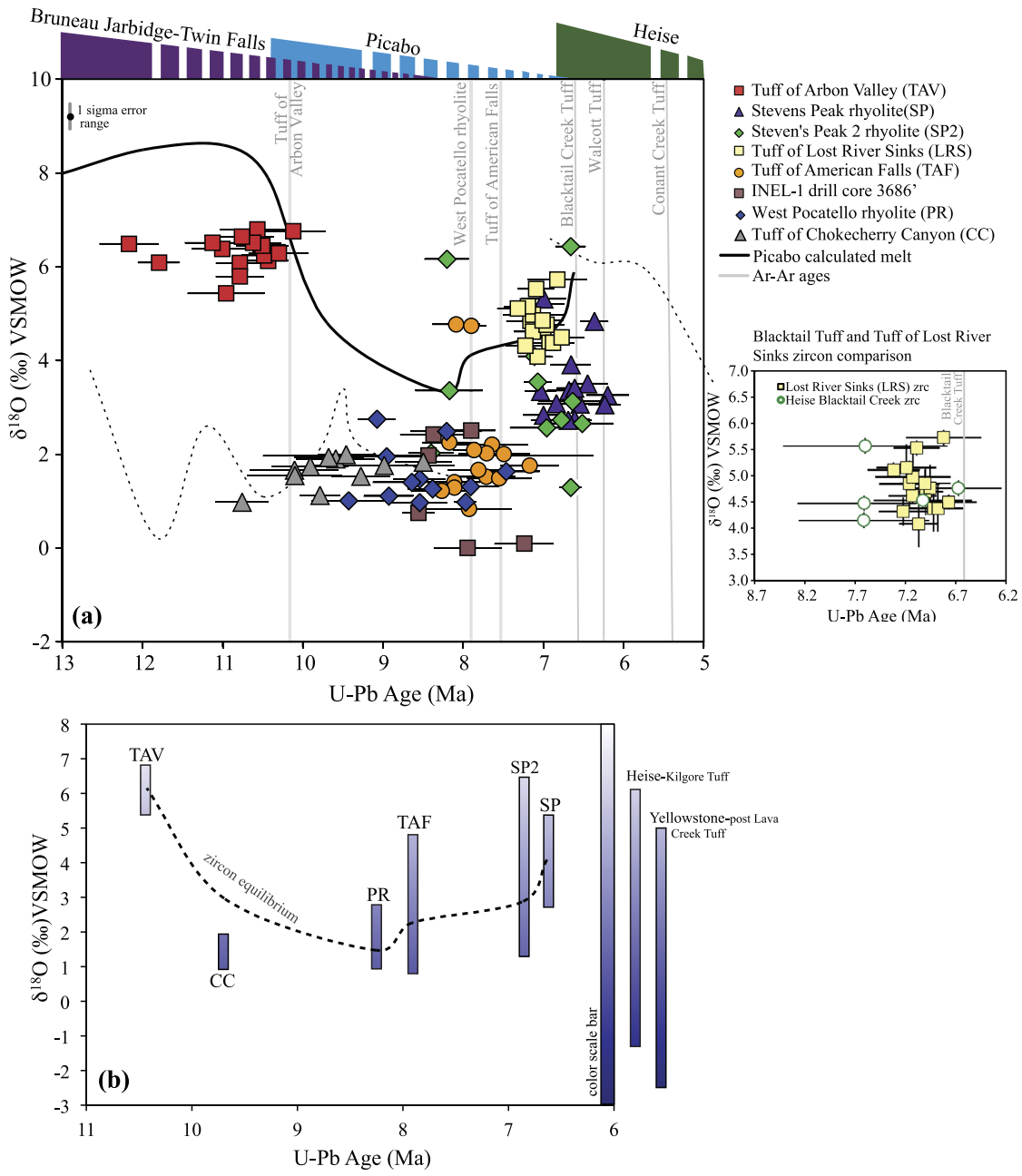

Fig. 6. a. Compilation of $\delta^{18}O$ compositions and U–Pb ages of individual zircons determined by ion microprobe. Calculated melt values are shown by the solid (Picabo) and dashed (Heise and Bruneau Jarbidge–Twin Falls) lines. Bruneau–Jarbidge/Twin Falls and Heise melt compositions are from Bonnichsen et al. (2008) and Watts et al. (2011), accordingly. Heise Ar–Ar ages are from Morgan and McIntosh (2005) and Picabo Ar–Ar ages (and K–Ar ages) are from Anders et al. (2009), Kellogg and Marvin (1988), and Kellogg et al. (1994), and are all shown by solid vertical gray lines. U–Pb age error bars are drawn at 1 standard error, and the $\delta^{18}O$ error bar reflects the weighted average of the standard errors (0.29 for 97 analyses). The colored bars at the top of the figure signify the approximate eruption duration of the three volcanic centers: Twin Falls, Picabo, and Heise, highlighting the presence of contemporaneous eruptions from different volcanic centers. The $\delta^{18}O$ melt curve is calculated from the $\delta^{18}O$ of major phenocrysts, plagioclase and quartz (same as Fig. 5). **b.** Summary of $\delta^{18}O$ zircon heterogeneity with average U–Pb age. Each bar corresponds to the range of $\delta^{18}O_{zircon}$ measured for each sample. The dotted line is the calculated zircon equilibrium $\delta^{18}O$, 1.8‰ less than the calculated melt $\delta^{18}O$, emphasizing the presence of disequilibrium zircons in the erupted rhyolites. Ranges of $\delta^{18}O_{zircon}$ for Heise and Yellowstone are derived from Watts et al. (2011) and Bindeman et al. (2008), respectively.

Without definitive evidence that caldera clusters existed during eruption of the first low-$\delta^{18}O$ rhyolite at Picabo, we search for alternative source rocks (other than buried and hydrothermally altered TAV) to be melted, and mechanisms (other than caldera collapse) to expedite hydrothermal alteration and melting. The possible source rocks include: (1) "Picabo" age intracaldera tuffs of 10.4–9.0 Ma that have not been identified near the surface, or in the INEL-1 borehole; (2) far-traveled ignimbrite units derived from the west, TF in particular, which preceded or were coeval with early Picabo volcanism; and (3) Eocene Challis volcanics.

These potential source rocks could be hydrothermally altered by low-$\delta^{18}O$ meteoric waters syneruption, during uplift and SRP plume-crust interaction, or during TAV caldera collapse. We include Challis as a potential source because Challis intrusives and volcanics: (1) are regionally abundant and exposed proximal to the Picabo volcanic field (Fig. 1a); (2) are already low-$\delta^{18}O$ in certain regions of Idaho due to syneruptive water-rock interaction (locally down to −8.8‰; Criss et al., 1991), however hydrothermal alteration is heterogeneous and sporadic; and (3) possess more primitive isotopic compositions (−3.5 to −19.7 $\varepsilon_{Hf}(0)$; Gaschnig et al.,

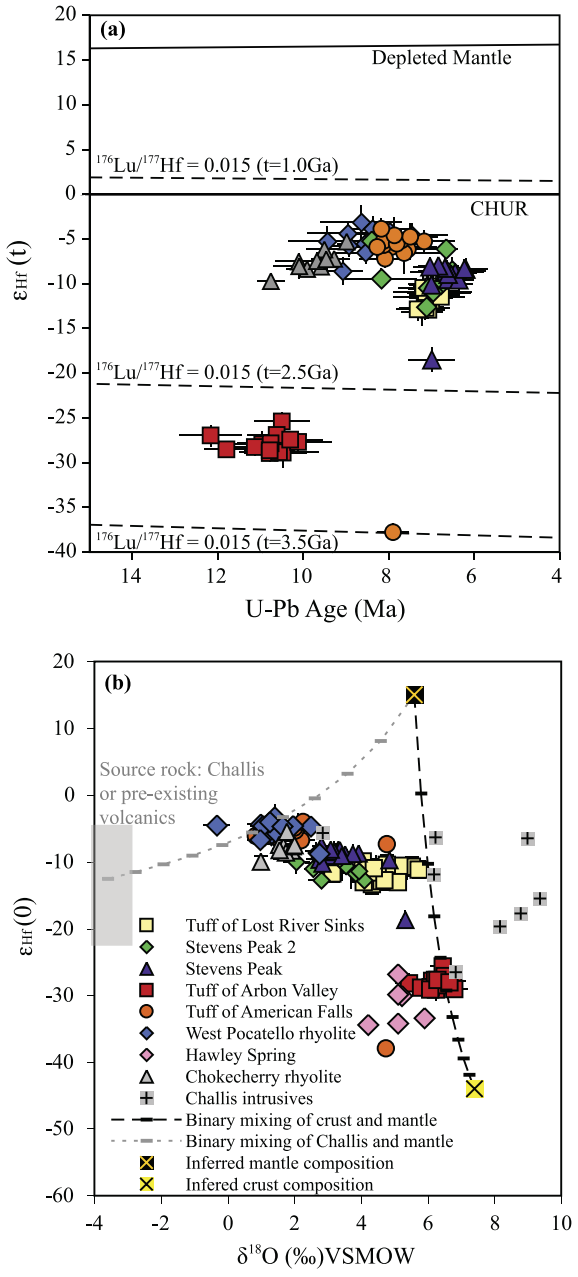

Fig. 7. a. $\varepsilon_{Hf}(t)$ versus U–Pb age of individual zircons from Picabo rhyolites with evolution lines of depleted mantle, CHUR (chondrite uniform reservoir) and average continental crust composition at various ages. One-sigma error bars are shown for the age and two-sigma error bars for $\varepsilon_{Hf}(t)$. **b.** $\varepsilon_{Hf}(0)$ versus $\delta^{18}O$ of individual zircons from Picabo rhyolites. The inferred crust composition is the average $\delta^{18}O$ of SRP xenoliths from Watts et al. (2010) and the average ε_{HF} of Archean crust worldwide (Vervoort and Patchett, 1996). The Challis field is approximated from average whole rock $\delta^{18}O$ of Challis volcanics (Criss et al., 1991) and whole rock ε_{HF} of Challis intrusives (Gaschnig et al., 2011). The low $\delta^{18}O$ Challis deposits range from 1.6 to −8.8‰, and although these values are not representative of the entire Challis deposit they serve as an end-member for low $\delta^{18}O$ Challis volcanics. The dotted lines are individual binary mixing models between the Challis and mantle (gray-dotted) and Archean crust and mantle (black-dashed) with individual tick marks corresponding to 10% increments. Two sigma error bars are shown for $\varepsilon_{Hf}(0)$ and one sigma error bars for $\delta^{18}O$.

2011) than the Archean crust or TAV (Fig. 4a, 7b). Thus, melting of the Challis volcanics inside of the collapsed TAV block (Fig. 8) would generate low-$\delta^{18}O$ Picabo volcanics without greatly impacting the Sr–Nd–Hf isotopic signature.

The proposed source rocks have the potential to constitute stratigraphically lower portions of the collapsed block and therefore would be closer to the heat source than intracaldera TAV for melting and generation of the first low-$\delta^{18}O$ magmas <1 m.y. after the TAV eruption. In this scenario, the purpose of the TAV caldera collapse is to create conditions for burial, further hydrothermal alteration, and melting without contributing mass. It is also likely that the 10.4 Ma TAV plutonic residuum was already fully crystalline by the time of voluminous low-$\delta^{18}O$ Picabo volcanism at ~9.7 Ma, and could therefore be cross-cut by the invading basalts to melt proposed sources in the intracaldera block.

An additional mechanism (other than caldera collapse) that would facilitate hydrothermal alteration and the juxtaposition of the proposed source rocks and heat source (required for melting) is Basin and Range extension (Fig. 8). We suggest that pre-modification of the crust due to Basin and Range extension, as well as SRP-plume driven extension would have allowed for hydrothermal alteration prior to caldera collapse. During Basin and Range extension, the formation of normal and detachment faults would down-drop the altered source units and provide additional heating and fracturing necessary to further elevate water-rock ratios, facilitating hydrothermal alteration in the upper crust. We advocate that the exhumation of metamorphic core complexes is one mechanism by which Basin and Range extension can facilitate hydrothermal alteration and production of low-$\delta^{18}O$ rhyolites. For example, exhumation of metamorphic core complexes has been specifically proposed for the Jim Sage Mts (Konstantinou et al., 2012), on the southern margin of the SRP between the Pocatello and TF volcanic fields (Fig. 1). Konstantinou (2011) describes the Jim Sage volcanics as being erupted from small eruptive centers along the Raft River Detachment-Albion Fault system, which exhumed the local metamorphic core complex, and proposed that associated faulting could have facilitated deep magma migration from the SRP. Konstantinou (2011) also allows for the possibility that the Jim Sage volcanics are associated with SRP volcanism. Although Basin and Range extension coeval with Picabo magmatism is not required to produce the rhyolites observed it would further facilitate the process and demonstrate the intertwined history of local tectonics and plume-driven magmatism in the SRP.

This model which we propose for "pre-modification" of the crust with respect to $\delta^{18}O$ applies to the CSRP (BJ-TF) and Picabo center where an overabundance of low $\delta^{18}O$ rhyolites are observed. However, caldera collapse is still an important pre-requisite to bring "pre-altered" source rocks closer to underlying heat sources, thus requiring the magma storage be shallow (Almeev et al., 2012). Our model has critical differences from the model proposed by Leeman et al. (2008), because we suggest that it is unlikely that: 1) water will travel up the temperature gradient; 2) water will remain isotopically unaffected on the descent to mid-crustal depths of 500–700 °C at 15 km; and 3) such great depths will have the necessary porosities for effective water-rock interaction. We postulate that in order to imprint significant low-$\delta^{18}O$ signatures on tens of thousands of cubic kilometers of source rocks (thousands of which are required to be melted to generate low-$\delta^{18}O$ SRP magmas), a fundamental two-stage process is required. First, shallow interaction between heated meteoric waters and source rocks with large porosities at high water-rock ratios; second, melting of these source rocks at depth following burial. A plume-derived heat source can induce shallow hydrothermal alteration and melting, which can be further facilitated by the heat supplied during exhumation of metamorphic core complexes. Therefore rift burial during Basin and Range extension and burial during caldera collapse can create conditions suitable for remelting of the surface-altered rocks.

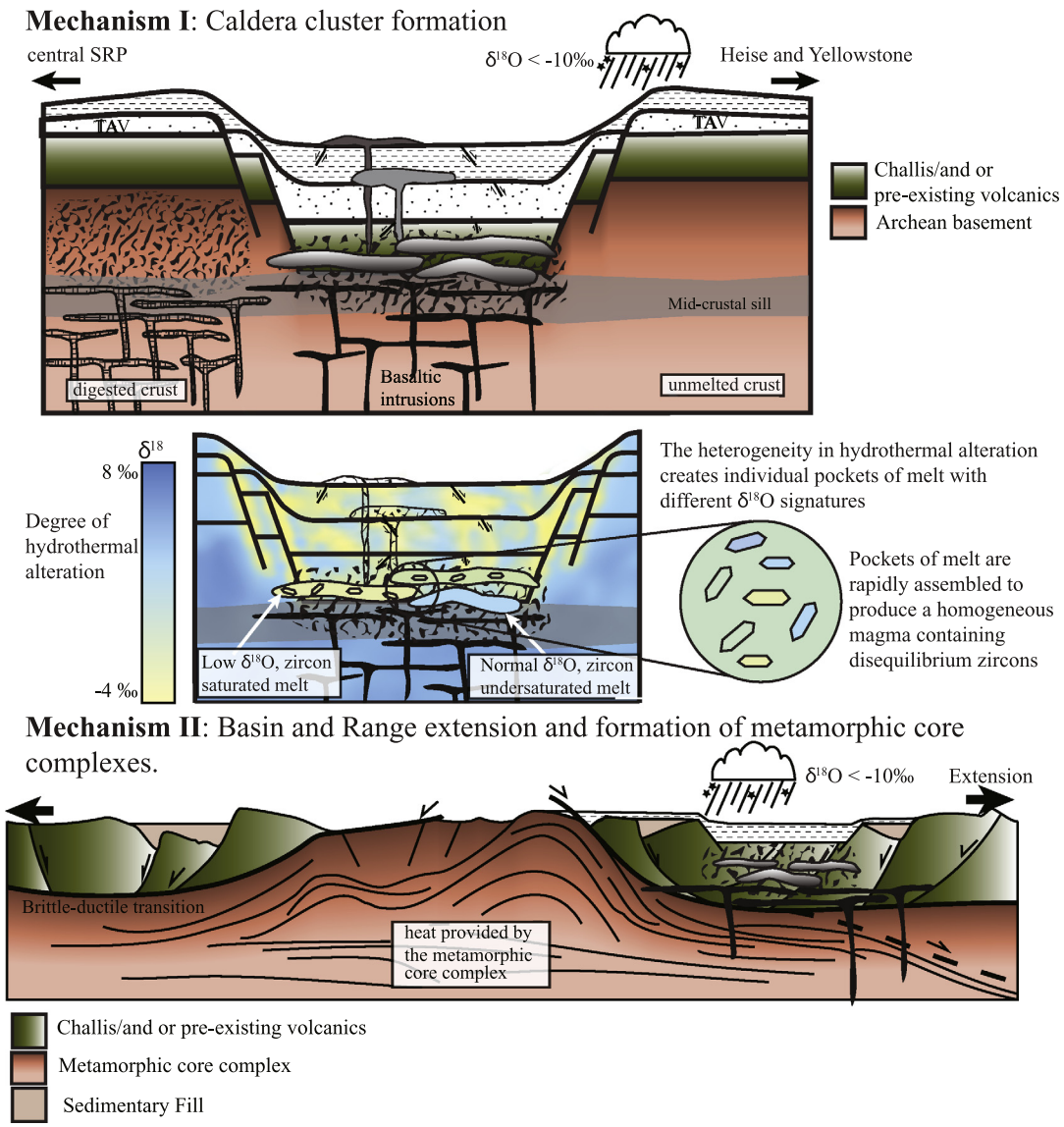

Fig. 8. Summary of the petrogenetic mechanisms proposed for generating low-δ^{18}O rhyolites at the Picabo volcanic field. The general features applicable to both mechanisms are a mid-crustal sill developing near the brittle-ductile transition of the crust, individual pockets of rhyolite melt forming from remelting gabbro with heat input from the pervasive basalt supply, alteration by low-δ^{18}O meteoric water, and generation of variable δ^{18}O signatures. Mechanism I demonstrates how repeated caldera formation results in the formation of a caldera cluster, and the progressive lowering of intracaldera rhyolite, bringing these units closer to basaltic intrusions (Bindeman and Valley, 2001; Watts et al., 2011). Hydrothermal alteration of buried deposits is shown by the blue to yellow gradient, emphasizing the heterogeneity of alteration we propose to be present. We also illustrate smaller lava flows between caldera forming eruptions that sample pockets of rhyolite melt with variable δ^{18}O compositions. As the North American plate migrates over the mantle plume, the crust, modified by basaltic intrusions, is progressively digested. Mechanism II demonstrates one example of how extensional tectonics of the Basin and Range can modify the crust and facilitate hydrothermal alteration. The exhumation of a metamorphic core complex is shown (modified from Rey et al., 2009), which facilitates hydrothermal alteration by extensive faulting coupled with the heat input from the intruded igneous and metamorphic rocks. The exhumation of this core complex causes a pre-modification of the crust with respect to δ^{18}O. (For interpretation of the references to color in this figure legend, the reader is referred to the web version of this article.)

5.4. Significance of zircon δ^{18}O diversity and Hf homogeneity in voluminous tuffs

The zircon heterogeneity, which we now observe at Picabo, suggests that isolated pockets of melt with unique δ^{18}O signatures were derived from variably altered volcanic predecessors and rapidly assembled prior to eruption. These individual pockets of melt were of variable temperature and zircon saturation, and therefore not all pockets of melt crystallized zircons. In order to preserve the observed O isotope diversity on a cm-scale these pockets of melt had to be thoroughly mixed prior to eruption. By retaining heterogeneous δ^{18}O signatures, many of the zircons are erupted in disequilibrium with the host melt. The lack of inherited zircons also implies that zircons dissolved and re-precipitated from these pockets of diverse δ^{18}O melt. In contrast to the heterogeneous zircon δ^{18}O, we observe homogeneous zircon Hf isotope signatures for all analyzed Picabo rhyolites. The presence of zircons diverse in δ^{18}O and homogeneous in ε_{Hf} (Fig. 11) suggests that the zircons crystallized after remelting variably hydrothermally-altered tuffs (affecting δ^{18}O, but not Hf), which themselves were already homogenized in whole rock ε_{Hf} isotopic composition during earlier magmatism and convection. The occasional low-ε_{Hf}(0) zircon xenocrysts indicate that Archean crust was added to the low-δ^{18}O magma chambers as well, but in small proportions (Fig. 10).

These diverse zircons and their host batches were assembled in a single reservoir and erupted without delay to prevent annealing by diffusion and solution-reprecipitation. We speculate that the process of rapid coalescence of individual (diverse in δ^{18}O) shal-

low magma batches may be the trigger for the caldera-forming eruptions, and could have occurred in response to an increased supply of basalt at the base of the magma chamber (e.g. Simakin and Bindeman, 2012). This increased supply of basalt could result in catastrophic magma assembly by merging individual magma batches, density destabilization of the caldera roof, and a caldera-forming eruption of low-δ^{18}O tuffs with diverse zircons.

5.5. Origin of silicic volcanism at the Picabo volcanic field and in the SRP

With the discovery of new rhyolites with diverse δ^{18}O compositions at the Picabo volcanic field it is now evident that nearly all SRP caldera clusters for the past ~16 Ma have produced voluminous low-δ^{18}O rhyolites, either at the end of caldera cluster evolution (Yellowstone, Heise), or throughout the eruptive sequence (CSRP). Picabo shares key similarities with Heise and Yellowstone, having produced initially normal-δ^{18}O magmas followed by voluminous low-δ^{18}O rhyolites in the later stages of caldera complex evolution. Like the voluminous low-δ^{18}O Kilgore Tuff of the Heise volcanic field (Watts et al., 2011), Picabo's low-δ^{18}O rhyolites (West Pocatello rhyolite, Tuff of Little Chokecherry Canyon, Tuff of American Falls, Stevens Peak, and Stevens Peak 2) possess diverse zircon populations. This transition from normal- to voluminous low-δ^{18}O rhyolites happens at all three centers after a ~2 Ma time delay from the onset of the first voluminous normal-δ^{18}O rhyolitic tuff eruption. At Picabo, <1 Ma separates eruption of the normal-δ^{18}O TAV from the low-δ^{18}O Tuff of Chokecherry Canyon. At Heise and Yellowstone, it appears that two to three nested caldera collapses are required to produce ~1000 km^3 of low-δ^{18}O rhyolites, therefore the predominance of low-δ^{18}O rhyolites at Picabo suggests that it shares similarities with the western eruptive centers, BJ–TF, whose exposed sections display overabundant low-δ^{18}O rhyolites with diverse zircons throughout the eruptive sequence. As we discussed above, these similarities suggest that a pre-modification of the crust was made possible in Basin and Range rift zones, and accelerated the process of low-δ^{18}O magma genesis at Picabo and volcanic fields to the west.

Another important result from our study is that there is significant spatiotemporal overlap between volcanism at TF–BJ, Picabo and Heise, indicating that eruptions at these various volcanic fields were contemporaneous during the transition between eruptive centers (Fig. 6a). However, the waning cycle of low-δ^{18}O volcanism in the BJ–TF centers, represented mostly by lavas (10.5–8 Ma), display universally low-δ^{18}O signatures (Bonnichsen et al., 2008; Boroughs et al., 2005; Ellis et al., 2010; Seligman, 2011), while the contemporaneous and newly developing Picabo center started with large-volume normal-δ^{18}O ignimbrite eruptions at 10.44 Ma. Likewise, the latest stages of volcanism at Picabo from 8.25–6.62 Ma were characterized by low-δ^{18}O values and diverse zircons, while the contemporaneous eruptions at Heise began with the normal-δ^{18}O Blacktail Creek Tuff with more homogeneous zircons (newly determined; Fig. 6a. inset). Late-stage low-δ^{18}O Picabo eruptions reached a maximum $\delta^{18}O_{melt}$ of 5.9‰, a close yet distinguishable δ^{18}O difference between the contemporaneous Heise and Picabo rhyolites.

Our new zircon U–Pb geochronology data also reveal a decreasing lifespan of each caldera complex across the Yellowstone hotspot track. Large-volume ignimbrite volcanism in the BJ–TF complexes spans ~12.8–10.5 Ma, followed by lavas as young as 6 Ma (Bonnichsen et al., 2008), thus BJ–TF has a lifespan of ~4–6 million yr. Picabo volcanism spans ~3.8 million yr (this study), Heise spans ~2.6 million yr (Watts et al., 2011) and Yellowstone spans ~2 million yr (Christiansen, 2001). Coupled with the decreasing lifespan is a decrease in the number of caldera-forming eruptions: BJ-TF (abundant, ~10–12), Picabo (~3–6), Heise (4) and Yellowstone (3). We interpret these spatiotemporal trends in eruption frequency and volcanism duration as reflecting a combination of the following: increasing thickness of the lithosphere from 40 km beneath TF to 47 km beneath Yellowstone (Yuan et al., 2010), and/or decreasing potency of the Yellowstone plume (Bonnichsen et al., 2008).

6. Conclusions

The Picabo eruptive center produced a series of voluminous rhyolites from 10.4–6.6 Ma that become progressively lower in magmatic δ^{18}O and more heterogeneous in zircon δ^{18}O through time. These trends are similar to what has been observed at Heise and Yellowstone, underscoring the importance of recycling hydrothermally altered intracaldera rhyolites at the end of caldera cluster evolution. In addition, similarities to BJ–TF suggest that coeval rifting, extension, and metamorphic core complex formation may further promote hydrothermal alteration and production of low-δ^{18}O source rocks. It now appears that at Picabo, Heise, and Yellowstone the eruption of ~1000 km^3 of low-δ^{18}O rhyolites with diverse zircon crystal cargoes heralds the end of caldera cluster evolution, and after volcanism initiates at a new location with normal δ^{18}O values and homogeneous zircon populations. The heterogeneous zircon population in late-stage low-δ^{18}O magmas supports our petrogenetic model that previously erupted tuffs and their subvolcanic roots were variably altered and lowered in δ^{18}O, and subsequently re-melted or "cannibalized" at the crustal-scale, causing the silicic crust to become more refractory and mafic. Our work also demonstrates the importance of large-scale batch assembly occurring on timescales more rapid than O isotope re-equilibration of zircons, but long enough to chemically homogenize the melt and δ^{18}O composition of phenocrysts. Picabo, is the third youngest volcanic field of the Yellowstone hotspot track, and the isotopic evolution of the suite of rhyolites we have studied contributes to our growing understanding of past and future magmatic activity at Yellowstone.

Acknowledgements

We thank Dylan Colon for analytical help and fieldwork assistance, Jim Palandri, Ben Ellis, Frank Ramos, Chris Fisher, and Jeff Vervoort for their analytical help, Les Kinsely for assistance with LA-MC-ICP-MS analysis, and Richard Gaschnig for contributing Challis intrusive samples. We also thank Calvin Miller, Jorge Vazquez, and an anonymous reviewer for their thoughtful reviews, which greatly helped to improve this paper. We also thank Angela Seligman for her help editing. This work was supported by NSF grant EAR/CAREER-844772, and the ion microprobe facility at UCLA utilized during this study is partly supported by a grant from the Instrumentation and Facilities Program, Division of Earth Sciences, National Science Foundation.

Appendix A. Supplementary material

Supplementary material related to this article can be found online at http://dx.doi.org/10.1016/j.epsl.2013.08.007.

References

Almeev, R., Bolte, T., Nash, B., Holtz, F., Erdmann, M., Cathey, H., 2012. High-temperature, low-H_2O silicic magmas of the Yellowstone hotspot: an experimental study of rhyolite from the Bruneau–Jarbidge Eruptive Center, Central Snake River Plain, USA. J. Petrol. 53 (9), 1837–1866.

Anders, M.H., Saltzman, J., Hackett, W.R., 1997. Borehole WO-2, the Rosetta stone (core) of the Heise volcanics of east central Idaho: implications for the track of the Yellowstone hotspot. Geol. Soc. Am. 29 (6), A–365.

Anders, M., Saltzman, J., Hemming, S., 2009. Neogene tephra correlations in eastern Idaho and Wyoming; Implications for Yellowstone hotspot-related volcanism and tectonic activity. Geol. Soc. Am. Bull. 121 (5–6), 837–856.

Armstrong, R.L., 1982. Cordilleran metamorphic core complexes; from Arizona to southern Canada. Annu. Rev. Earth Planet. Sci. 10, 129–154.

Armstrong, R.L., Ward, P.L., 1991. Evolving geographic patterns of Cenozoic magmatism in the North American Cordillera: The temporal and spatial association of magmatism and metamorphic core complexes. J. Geophys. Res. 96 (B8), 13201–13224.

Best, M.G., Christiansen, E.H., 1991. Limited extension during peak Tertiary volcanism, Great Basin of Nevada and Utah. J. Geophys. Res. 96 (B8), 13509–13528.

Bindeman, I.N., 2008. Oxygen isotopes in mantle and crustal magmas as revealed by single crystal analysis. In: Putirka, K.D., Tepley III, F.J. (Eds.), Minerals, Inclusions and Volcanic Processes. In: Rev. Mineral. Geochem., vol. 69. Mineralogical Society of America and Geochemical Society, pp. 445–478.

Bindeman, I.N., Valley, J., 2001. Low-^{18}O rhyolites from Yellowstone: Magmatic evolution based on analyses of zircons and individual phenocrysts. J. Petrol. 42 (8), 1491–1517.

Bindeman, I.N., Valley, J.W., 2003. Rapid generation of both high- and low-δ^{18}O, large-volume silicic magmas at the Timber Mountain/Oasis Valley caldera complex, Nevada. Geol. Soc. Am. Bull. 115 (5), 581–595.

Bindeman, I.N., Watts, K.E., Schmitt, A.K., Morgan, L.A., Shanks, P.W.C., 2007. Voluminous low-δ^{18}O magmas in the late Miocene Heise volcanic field, Idaho: Implications for the fate of Yellowstone hotspot calderas. Geology 35 (11), 1019–1022.

Bindeman, I.N., Fu, B., Kita, N.T., Valley, J.W., 2008. Origin and evolution of silicic magmatism at Yellowstone based on ion microprobe analysis of isotopically zoned zircons. J. Petrol. 49 (1), 163–193.

Bonnichsen, B., Leeman, W.P., Honjo, N., McIntosh, W.C., Godchaux, M.M., 2008. Miocene silicic volcanism in southwestern Idaho: geochronology, geochemistry, and evolution of the central Snake River Plain. Bull. Volcanol. 70 (3), 315–342.

Boroughs, S.B., Wolff, J.A., Bonnichsen, B., Godchaux, M., Larson, P., 2005. Large volume, low-δ^{18}O rhyolites of the central Snake River Plain, Idaho, USA. Geology 33, 821–824.

Boroughs, S., Wolff, J.A., Ellis, B.S., Bonnichsen, B., Larson, P., 2012. Evaluation of models for the origin of Miocene low-δ^{18}O rhyolites of the Yellowstone/Columbia River Large Igneous Province. Earth Planet. Sci. Lett. 313–314, 45–55.

Branney, M.J., Bonnichsen, B., Andrews, G.D.M., Ellis, B., Barry, T.L., McCurry, M., 2008. "Snake River (SR)-type" volcanism at the Yellowstone hotspot track: distinctive products from unusual, high-temperature silicic super-eruptions. Bull. Volcanol. 70 (3), 293–314.

Burchfiel, B.C., Cowan, D.S., Davis, G.A., 1992. Tectonic overview of the Cordilleran Orogen in the western United States. In: Burchfiel, C., et al. (Eds.), The Cordilleran Orogen: Conterminous, vol. G-3. Geol. Soc. Am., Geology of North America, U.S., Boulder. Colorado, pp. 407–480.

Camp, V.E., Hanan, B.B., 2008. A plume-triggered delamination origin for the Columbia River Basalt Group. Geosphere 4 (3), 480–495.

Cathey, H.E., Nash, B.P., 2004. The Cougar Point Tuff: implications for thermochemical zonation and longevity of high-temperature, large-volume silicic magmas of the Miocene Yellowstone hotspot. J. Petrol. 45 (1), 27–58.

Cathey, H.E., Nash, B.P., 2009. Pyroxene thermometry of rhyolite lavas of the Bruneau–Jarbidge eruptive center, Central Snake River Plain. J. Volcanol. Geotherm. Res. 188, 173–185.

Cathey, H.E., Nash, B.P., Allen, C.M., Campbell, I.H., Valley, J.W., Kita, N., 2008. U–Pb zircon geochronology and Ti-in-zircon thermometry of large-volume low-δ^{18}O magmas of the Miocene Yellowstone hotspot. Geochim. Cosmochim. Acta 72, A143.

Christiansen, R.L., 2001. The Quaternary and Pliocene Yellowstone Plateau Volcanic Field of Wyoming, Idaho, and Montana. U.S. Geol. Surv. Professional Papers 729-G, 1–145.

Christiansen, E., McCurry, M., 2008. Contrasting origins of Cenozoic silicic volcanic rocks from the western Cordillera of the United States. Bull. Volcanol. 70 (3), 251–267.

Christiansen, R.L., Yeats, R.S., 1992. Post-Laramide geology of the U.S. Cordilleran region. In: Burchfiel, B.C., et al. (Eds.), The Cordilleran Orogen: Conterminous, vol. G-3. Geol. Soc. Am. Geology of North America, U.S., Boulder. Colorado, pp. 261–406.

Colgan, J.P., Henry, C.D., 2009. Rapid middle Miocene collapse of the Mesozoic orogenic plateau in north central Nevada. Int. Geol. Rev. 51, 20–961.

Colgan, J.P., Shuster, D.L., Reiners, P., 2007. Two-phase Neogene extension of the northwestern Basin and Range deduced from thermochronology of a single sample. Eos 88, V33E-06 (Transactions, American Geophysical Union).

Coney, P.J., 1980. Cordilleran metamorphic core complexes: An overview. In: Crittenden Jr., D., et al. (Eds.), Cordilleran Metamorphic Core Complexes. Geol. Soc. Am. Mem. 153, 7–31.

Covington, H.R., 1983. Structural evolution of the Raft River Basin, Idaho; Tectonic and stratigraphic studies in the eastern Great Basin. In: Miller, D.M., et al. (Eds.), Tectonic and Stratigraphic Studies in the Eastern Great Basin. Geol. Soc. Am. Mem. 157, 229–237.

Criss, R.E., Fleck, R.J., 1987. Petrogenesis, geochronology, and hydrothermal systems in the northern Idaho batholith and adjacent areas based on ^{18}O/^{16}O, D/H, ^{87}Sr/^{86}Sr, K-Ar, and ^{40}Ar/^{39}Ar studies. U.S. Geol. Surv. Professional Papers 1436, 95–137.

Criss, R., Fleck, R., Taylor, H., 1991. Tertiary meteoric hydrothermal systems and their relation to ore deposition, northwestern United States and southern British Columbia. J. Geophys. Res. 96 (B8), 13335–113356.

DeCelles, P.G., 1994. Late Cretaceous-Paleocene synorogenic sedimentation and kinematic history of the Sevier thrust belt, northeast Utah and southwest Wyoming. Geol. Soc. Am. Bull. 106, 32–56.

DeCelles, P.G., 2004. Late Jurassic to Eocene evolution of the Cordilleran thrust belt and foreland basin system, western U.S.A. Am. J. Sci. 304, 105–168.

Doherty, D. McBroome, L. Kuntz, M., 1979. Preliminary geological interpretation and lithologic log of the exploratory geothermal test well (INEL-1) Idaho National Engineering Laboratory, Eastern Snake River Plain, Idaho. Open-File Report, U.S. Geol. Surv.

Egger, A.E., Glen, J.M., Ponce, D.A., 2010. The northwestern margin of the Basin and Range province. Part 2: Structural setting of a developing basin from seismic and potential field data. Tectonophysics 488, 150–161.

Egger, A.E., Dumitru, T.A., Miller, E.L., Savage, C.F.I., Wooden, J.L., 2003. Timing and nature of Tertiary plutonism and extension in the Grouse Creek Mountains, Utah. Int. Geol. Rev. 45, 497–532.

Eggins, S.M., Grün, R., McCulloch, M.T., Pike, A.W.G., Chappell, J., Kinsley, L., Mortimer, G., Shelley, M., Murray-Wallace, C.V., Spötle, C., Taylor, L., 2005. In situ U-series dating by laser-ablation multi-collector ICPMS: new prospects for Quaternary geochronology. Quat. Sci. Rev. 24, 2523–2538.

Ellis, B.S., Barry, T., Branney, M.J., Wolff, J.A., Bindeman, I., Wilson, R., Bonnichsen, B., 2010. Petrologic constraints on the development of a large-volume, high temperature, silicic magma system: The Twin Falls eruptive centre, central Snake River Plain. Lithos 120 (3–4), 475–489.

Farmer, G.L., Depaolo, D.J., 1983. Origin of Mesozoic and Tertiary granite in the western United States and implications for Mesozoic crustral structure: 1. Nd and Sr isotopic studies in the geocline of the northern Great Basin. J. Geophys. Res. 88, 3379–3401.

Fleck, R.J., Criss, R.E., 1985. Strontium and oxygen isotopic variations in Mesozoic and Tertiary plutons of central Idaho. Contrib. Mineral. Petrol. 90, 291–308.

Fosdick, J.C., Colgan, J.P., 2008. Miocene extension in the east range, Nevada; a two-stage history of normal faulting in the northern Basin and Range. Geol. Soc. Am. Bull. 120, 1198–1213.

Foster, D.A., Fanning, C.M., 1997. Geochronology of the northern Idaho Batholith and the Bitterroot metamorphic core complex; magmatism preceding and contemporaneous with extension. Geol. Soc. Am. Bull. 109, 379–394.

Foster, D.A., Grice Jr., W.C., Kalakay, T.J., 2010. Extension of the Anaconda metamorphic core complex: ^{40}Ar/^{39}Ar thermochronology and implications for Eocene tectonics of the northern Rocky Mountains and the Boulder batholith. Lithosphere 2, 232–246.

Foster, D.A., Doughty, P.T., Kalakay, T.J., Fanning, C.M., Coyner, S., Grice Jr., W.C., Vogl, J.J., 2007. Kinematics and timing of exhumation of Eocene metamorphic core complexes along the Lewis and Clark fault zone, northern Rocky Mountains, USA, in exhumation along Major Continental Strike-Slip systems. Spec. Pap., Geol. Soc. Am. 434, 205–229.

Gans, P.B., 1987. An open-system, two-layer crustal stretching model for the eastern Great Basin. Tectonics 6, 1–12.

Gaschnig, R., Vervoort, J., Lewis, R., Tikoff, B., 2011. Isotopic Evolution of the Idaho Batholith and Challis Intrusive Province, Northern US Cordillera. J. Petrol. 52 (12), 2397–2429.

Graham, D.W., Reid, M.R., Jordan, B.T., Grunder, A.L., Leeman, W.P., Lupton, J.E., 2009. Mantle source provinces beneath the Northwestern USA delimited by helium isotopes in young basalts. J. Volcanol. Geotherm. Res. 188 (1–3), 128–140.

Hanchar, J., Watson, E., 2003. Zircon saturation thermometry. Rev. Mineral. Geochem. 53, 89–112.

Hildreth, W., Halliday, A.N., Christiansen, R.L., 1991. Isotopic and chemical evidence concerning the genesis and contamination of basaltic and rhyolitic magmas beneath the Yellowstone Plateau Volcanic Field. J. Petrol. 32, 63–138.

Hughes, S., McCurry, M., Geist, D., 2002. Geochemical correlations and implications for the magmatic evolution of basalt flow groups at the Idaho National Engineering and Environmental Laboratory. Geol. Soc. Am. 353, 151–173.

Kellogg, K.S., Marvin, R.F., 1988. New potassium-argon ages, geochemistry, and tectonic setting of upper cenozoic volcanic rocks near blackfoot Idaho. U.S. Geol. Surv. Bull. 1806, 1–19.

Kellogg, K.S., Harlan, S.S., Mehnert, H.H., Snee, L.W., Pierce, K.L., Hackett, W.R., Rodgers, D.W., 1994. Major 10.2 Ma rhyolitic volcanism in the eastern Snake River Plain, Idaho-Isotopic age and stratigraphic setting of the Arbon Valley Tuff Member of the starlight formation. U.S. Geol. Surv. Bull. 2091, 1–18.

King, E., Valley, J., 2001. The source, magmatic contamination, and alteration of the Idaho batholith. Contrib. Mineral. Petrol. 142 (1), 72–88.

Konstantinou, A., 2011. Off-axis Snake River plain magmatism along an active extensional detachment: An example from the Jim Sage volcanic suite, southern ID. Geol. Soc. Am. 43 (5), 106.

Konstantinou, A., Strickland, A., Miller, E., Wooden, J., 2012. Multistage Cenozoic extension of the Albion–Raft River–Grouse Creek metamorphic. core complex; geochronologic and stratigraphic constraints. Geosphere 8 (6), 1429–1466.

Kuntz, M.A., Covington, H.R., Schorr, L.J., 1992. An overview of basaltic volcanism of the eastern Snake River Plain, Idaho. In: Link, P.K., Kuntz, M.A., Platt, L.P. (Eds.), Regional Geology of Eastern Idaho and Western Wyoming. Geol. Soc. Am. Mem. 179, 227–267.

Leeman, W., Annen, C., Dufek, J., 2008. Snake River Plain-Yellowstone silicic volcanism; implications for magma genesis and magma fluxes. Geol. Soc. Am. Spec. Pub. 304, 235–259.

Leeman, W.P., Menzies, M.A., Matty, D.J., Embree, G.F., 1985. Strontium, neodymium and lead isotopic compositions of deep crustal xenoliths from the Snake River Plain: Evidence for Archean basement. Earth Planet. Sci. Lett. 75, 354–368.

McCurry, Michael, 2009. The Arbon Valley Tuff: A new look at a highly anomalous ignimbrite from the Yellowstone–Snake River Plain track. Geol. Soc. Am. 41 (6), 43.

McCurry, M., Rodgers, D.W., 2009. Mass transfer along the Yellowstone hotspot track I: Petrologic constraints on the volume of mantle-derived magma. J. Volcanol. Geotherm. Res. 188 (1–3), 86–98.

Miller, C., Meschter McDowell, S., Mapes, R., 2003. Hot and cold granites? Implications of zircon saturation temperatures and preservation of inheritance. Geology 31 (6), 529–532.

Miller, E.L., Dumitru, T.A., Brown, R.W., Gans, P.B., 1999. Rapid Miocene slip on the Snake Range–Deep Creek Range fault system, east-central Nevada. Geol. Soc. Am. Bull. 111, 886–905.

Morgan, L., Doherty, D., Leeman, W., 1984. Ignimbrites of the eastern Snake River Plain: Evidence for major caldera-forming eruptions. J. Geophys. Res. 89 (B10), 8665–8678.

Morgan, L.A., McIntosh, W.C., 2005. Timing and development of the Heise volcanic field, Snake River Plain, Idaho, western USA. Geol. Soc. Am. Bull. 117 (3), 288–306.

Nash, B., Perkins, M., 2012. Neogene Fallout Tuffs from the Yellowstone Hotspot the Columbia Plateau Region Oregon, Washington and Idaho, USA. PLoS ONE 7, 1–13.

Nash, B., Perkins, M., Christensen, J., Lee, D., Halliday, A., 2006. The Yellowstone hotspot in space and time: Nd and Hf isotopes in silicic magmas. Earth Planet. Sci. Lett. 247 (1–2), 143–156.

Norman, M.D., Mertzman, S.A., 1991. Petrogenesis of Challis volcanics form central and southwestern Idaho: Trace element and Pb isotopic evidence. J. Geophys. Res. 96 (B8), 13279–13293.

Orr, W.N., Orr, E.L., 1996. Central Idaho and Snake River Plain and Owyhee Uplands. In: Geology of the Pacific Northwest. McGraw-Hill Co., New York, NY, pp. 160–211.

Paton, C., Hellstrom, J., Paul, B., Woodhead, J., Hergt, J., 2011. Iolite: Freeware for the visualisation and processing of mass spectrometric data. J. Anal. At. Spectrom. 26, 2508–2518.

Pearce, J.A., Harris, N.B., Tindle, A.G., 1984. Trace element discrimination diagrams for the tectonic interpretation of granitic rocks. J. Petrol. 25, 956–983.

Pierce, K.L., Covington, H.R., Williams, P.L., McIntyre, D.H., 1983. Geologic map of the Cotterel Mountains and the northern Raft River valley, Cassia County, Idaho. U.S. Geol. Surv. Miscellaneous Investigations I-1450.

Pierce, K., Morgan, L., 1992. The track of the Yellowstone hot spot: Volcanism, faulting, and uplift. Geol. Soc. Am. Mem. 179, 1–53.

Pope, A.D., 2002. Geology of the Wakley Peak, Idaho, 7.5' Quadrangle: Multiple phases of Late Miocene to Pliocenel extension, and relations to the southern Hawkins basin volcanic center. Idaho State University (M.S.).

Rey, P.F., Teyssier, C., Whitney, D.L., 2009. The role of partial melting and extensional strain rates in the development of metamorphic core complexes; orogens. Hot. Tectonophysics 477, 135–144.

Rodgers, D., McCurry, M., 2009. Mass transfer along the Yellowstone hotspot track II: Kinematic constraints on the volume of mantle-derived magma. J. Volcanol. Geotherm. Res. 188 (1–3), 99–107.

Schmandt, B., Dueker, K., Humphreys, E., Hansen, S., 2012. Hot mantle upwelling across the 660 beneath Yellowstone. Earth Planet. Sci. Lett. 331–332, 224–236.

Seligman, A.N., 2011. Generation of low-δ^{18}O silicic magmas, Bruneau Jarbidge volcanic center, Yellowstone hotspot: Evidence from zircons, including oxygen isotopes, U–Th–Pb dating, and melt inclusions. The University of Utah (M.S.).

Shervais, J.W., Vetter, S.K., Hanan, B.B., 2006. Layered mafic sill complex beneath the eastern Snake River Plain: evidence from cyclic geochemical variations in basalt. Geology 34 (5), 365–368.

Simakin, A.G., Bindeman, I.N., 2012. Remelting in caldera and rift environments and the genesis of hot, "recycled" rhyolites. Earth Planet. Sci. Lett. 337–338, 224–235.

Stockli, D.F., 1999. Regional timing and spatial distribution of miocene extension the northern Basin and Range Province. Ph.D. Stanford University.

Trail, D., Mojzsis, S.J., Harrison, T.M., Schmitt, A.K., Watson, E.B., Young, E.D., 2007. Constraints on Hadean zircon protoliths from oxygen isotopes, Ti-thermometry, and rare earth elements. Geochem. Geophys. Geosyst. 8 (6), 1–22.

Valley, J.W., 2003. Oxygen isotopes in zircon. In: Hanchar, J.M., Hoskin, P.W.O. (Eds.), Zircon. Rev. Mineral. Geochem., vol. 53. Mineralogical Society of America, pp. 343–385.

Valley, J.W., Bindeman, I.N., Peck, W.H., 2003. Empirical calibration of oxygen isotope fractionation in zircon. Geochim. Cosmochim. Acta 67 (17), 3257–3266.

Vazquez, J.A., Reid, M.R., 2002. Time scales of magma storage and differentiation of voluminous high-silica rhyolites at Yellowstone caldera Wyoming. Contrib. Mineral. Petrol. 144, 274–285.

Vervoort, J.D., Patchett, P.J., 1996. Behavior of Hafnium and Neodymium Isotopes in the Crust: Constrains from Precambrian crustally derived granites. Geochim. Cosmochim. Acta 60 (19), 3717–3733.

Watts, K.E., Bindeman, I.N., Schmitt, A.K., 2011. Large-volume rhyolite genesis in caldera complexes of the Snake River Plain: Insights from the Kilgore Tuff of the Heise Volcanic Field, Idaho, with comparison to Yellowstone and Bruneau–Jarbidge rhyolites. J. Petrol. 52 (5), 857–890.

Watts, K.E., Bindeman, I.N., Schmitt, A.K., 2012. Crystal scale anatomy of a dying supervolcano: an isotope and geochronology study of individual phenocrysts from voluminous rhyolites of the Yellowstone caldera. Contrib. Mineral. Petrol. 164, 45–67.

Watts, K.E., Leeman, W.P., Bindeman, I.N., Larson, P.B., 2010. Supereruptions of the Snake River Plain: Two-stage derivation of low-δ^{18}O rhyolites from normal-δ^{18}O crust as constrained by Archean xenoliths. Geology 38, 503–506.

Wells, M.L., Hoisch, T.D., 2008. The role of mantle delamination in widespread Late Cretaceous extension and magmatism in the Cordilleran orogen, western United States. Geol. Soc. Am. Bull. 120, 515–530.

Wells, M.L., Snee, L.W., Blythe, A.E., 2000. Dating of major normal fault systems using thermochronology; an example from the Raft River detachment, Basin and Range, western United States. J. Geophys. Res. 105 (B7), 16303–16327.

Whitehead, R.L., 1992. Geohydrologic framework of the Snake River Plain aquifer system, Idaho and Eastern Oregon. U.S. Geol. Surv. Professional Paper 1408-B.

Woodhead, J., Hergt, J., Shelley, M., Eggins, S., Kemp, R., 2004. Zircon Hf-isotope analysis with an excimer laser, depth profiling, ablation of complex geometries, and concomitant age estimation. Chem. Geol. 209, 121–135.

Yuan, H., Dueker, K., Stachnik, J., 2010. Crustal structure and thickness along the Yellowstone hot spot track: Evidence for lower crustal outflow-from beneath the eastern Snake River Plain. Geochem. Geophys. Geosyst. 11 (3), 1–14.